Extended Kalman Filter for Spacecraft Pose Estimation Using Dual Quaternions

Nuno Filipe,* Michail Kontitsis,† and Panagiotis Tsiotras‡

Georgia Institute of Technology, Atlanta, GA 30332-0150

Based on the highly successful Quaternion Multiplicative Extended Kalman Filter (Q-MEKF) for spacecraft attitude estimation using unit quaternions, this paper proposes a Dual Quaternion Multiplicative Extended Kalman Filter (DQ-MEKF) for spacecraft pose (i.e., attitude and position) and linear and angular velocity estimation using unit dual quaternions. By using the concept of error unit dual quaternion, defined analogously to the concept of error unit quaternion in the Q-MEKF, this paper proposes, as far as the authors know, the first multiplicative EKF for pose estimation. The state estimate of the DQ-MEKF can directly be used by recently proposed pose controllers based on dual quaternions, without any additional conversions, thus providing an elegant solution to the output dynamic compensation problem of the full 6DOF motion of a rigid body. Three formulations of the DQ-MEKF are presented. The first takes continuous-time linear and angular velocity measurements with noise and bias and discrete-time pose measurements with noise. The second takes only discrete-time pose measurements with noise and, hence, is suitable for satellite proximity operation scenarios where the chaser satellite has only access to measurements of the relative pose, but requires the relative linear and angular velocities for control. The third formulation takes continuous-time angular velocity and linear acceleration measurements with noise and bias and discrete-time pose measurements with noise. The proposed DQ-MEKF is compared with two alternative EKF formulations on a 5-DOF air-bearing platform and through extensive Monte-Carlo simulations.

*Ph.D. Candidate, School of Aerospace Engineering, AIAA Student Member. Email: nuno.filipe@gatech.edu

†Postdoctoral Research Associate, School of Aerospace Engineering.

‡Dean's Professor, School of Aerospace Engineering, AIAA Fellow.

I. Introduction

The highly successful Quaternion Multiplicative Extended Kalman Filter (Q-MEKF) based on unit quaternions for spacecraft attitude estimation, described in detail in Section XI of Ref. [1], has been used extensively in several NASA spacecraft.[2] It has been analyzed in great detail throughout the years.[3–6] Part of the Q-MEKF success lies on the fact that unit quaternions provide a global non-singular representation of attitude with the minimum number of parameters. Moreover, they appear linearly in the kinematic equations of motion, unlike Euler angles which require the calculation of computationally expensive trigonometric functions. Although newer approaches, such as nonlinear observers, have been shown to have some advantages over the classical EKF, a comprehensive survey of nonlinear attitude estimation methods has concluded that the classical EKF is still the most useful and practical solution to the attitude estimation problem.[2] Note that the lack of success of Kalman filtering before 1967, when Richard Battin was developing Apollo's on-board navigation and guidance system, is mainly attributed to the inability to model the system dynamics accurately enough.[1]

An additional major advantage of the Q-MEKF is that the 4-by-4 covariance matrix of the four elements of the unit quaternion does not need to be computed. As stated in Ref. [1], propagating this covariance matrix is the largest computational burden in any Kalman filter implementation. By rewriting the state of the EKF in terms of the three elements of the vector part of the unit *error* quaternion between the true unit quaternion and its estimate, only a 3-by-3 covariance matrix needs to be computed. The unavoidable drawback of this approach is that all three-dimensional attitude representations are singular or discontinuous for certain attitudes.[4] Indeed, by construction, the Q-MEKF described in Section XI of Ref. [1] will fail if the attitude error between the true attitude and its estimate is larger than 180 deg. However, unlike the true attitude of the body which can vary arbitrarily, the attitude error between the true attitude of the body and its estimate is expected to be close to zero, especially after the Q-MEFK has converged. Hence, in the Q-MEKF, whereas the attitude covariance matrix is only 3-by-3, the body can still have any arbitrary attitude. This is one of the most appealing properties of the Q-MEKF. Note that the 180 deg restriction in Q-MEKF is benign since the Q-MEKF will most likely fail even before the attitude *error* reaches 180 deg, due to the linearization assumptions intrinsic to the EKF.

The vector part of a unit quaternion is only one of several possible three-dimensional representations of the attitude error in the Q-MEKF.[4] Other possible representations are, for example, the rotation vector, the Rodrigues parameters, or the modified Rodrigues parameters. These representations have been shown to be equivalent up to third-order and, hence, are equivalent for the EKF and second-order filters.[4] In this paper, the attitude error

is represented using the vector part of a unit quaternion as in Ref. [1]. For a thorough discussion of the pros and cons of each representation, the reader is referred to Ref. [4]. Note however that, as mentioned above, all three-dimensional attitude representations are singular or discontinuous for certain attitudes.[4]

Recently, Refs. [7, 8], have proposed a new method to develop pose controllers starting from existing attitude-only controllers by utilizing the transfer principle between quaternion and dual quaternion descriptions.[9] In particular, unit dual quaternions offer a compact representation of the position and attitude of a frame with respect to another frame. Their properties, including examples of previous applications, are discussed in length in Ref. [8]. However, the property that makes dual quaternions most appealing for the applications we are interested in, is that the combined translational and rotational kinematic and dynamic equations of motion when written in terms of dual quaternions have the same form as the rotational-only kinematic and dynamic equations of motion written in terms of quaternions (albeit the operations have now to be interpreted in *dual* quaternion algebra).

The traditional approach to estimate the pose of a body consists on developing separate estimators for attitude and position. For example, Ref. [10] suggests two discrete-time linear Kalman filters to estimate the relative attitude and position separately. Since the translation Kalman filter requires the attitude estimated by the rotation Kalman filter, the former is only switched on after the latter has converged. Owing to this inherent coupling between rotation and translation, several authors have proposed estimating the attitude and position simultaneously. For example, in Ref. [11], a lander's terrain-relative position and attitude are estimated simultaneously using an EKF. The state of the EKF contains the vector part of the unit error quaternion (like in the Q-MEKF) and the position vector of the lander with respect to the inertial frame expressed in the inertial frame. In Ref. [12] the relative position and attitude of two satellites are also estimated simultaneously using an EKF. In this case, the state of the EKF contains the vector part of the unit error quaternion (like the Q-MEKF) and the position vector of the chaser satellite with respect to the target satellite expressed in a reference frame attached to the target satellite. The approach described in Ref. [12] is cooperative, in the sense that the two satellites share their angular velocity measurements. Finally, Ref. [13] also estimates the position and attitude between two frames simultaneously using a discrete-time EKF. In Ref. [13], the state contains the position vector of a body with respect to some reference frame expressed in that reference frame along with the four elements of the true quaternion describing the orientation of the body. Hence, Reference [13] does not take advantage of the concept of unit error quaternion. Moreover, in Ref. [13], the optimal Kalman state update is added to, and not multiplied with, the current best unit quaternion estimate, making the EKF presented in Ref. [13] additive instead of multiplicative. Below we elaborate why a multiplicative error description is more appropriate for this problem.

Reference [13] takes advantage of the compactness of dual quaternions to represent 3-D lines (and their relative position and orientation) to develop the measurement update of the EKF.

As far as the authors know, the only previous EKF formulations where the state includes a unit dual quaternion are given in Refs. [14, 15]. However, these EKF formulations include the true unit dual quaternion describing the pose of the body and not the error unit dual quaternion between the true unit dual quaternion and its best estimate. Therefore, the state of the EKF formulations presented in Refs. [14,15] contains all eight elements of the unit dual quaternion. Moreover, the EKF formulations proposed in Refs. [14, 15] are additive EKF formulations, i.e., the optimal Kalman state update is added to and not multiplied with the current best unit dual quaternion estimate. As a consequence, the predicted value of the unit dual quaternion immediately after a measurement update does not fulfill the two algebraic constraints that a unit dual quaternion must satisfy. Hence, in Ref. [14], the predicted value after a measurement update is further modified to satisfy these constraints through a process that includes parameters that must be tuned by the user. On the other hand, in Ref. [15], these two algebraic constraints are simply not enforced after a measurement update, which can lead to numerical problems. Finally, it should be mentioned that the discrete-time EKF formulations in Refs. [14, 15] are designed to take only measurements from a camera.

Compared to the existing literature, the main contributions of this paper are:

1) By using the concept of *error unit dual quaternion* defined analogously to the concept of error unit quaternion of the Q-MEKF, this paper proposes, as far as the authors know, the first multiplicative EKF for pose estimation. As a consequence, the predicted value of the unit dual quaternion immediately after a measurement update automatically satisfies the two algebraic constraints of a unit dual quaternion. Unlike in Ref. [14], no additional parameters need to be tuned by the user.
2) By using the error unit dual quaternion instead of the true unit dual quaternion, the state of the DQ-MEKF is reduced from eight elements (as in Refs. [14, 15]) to just six. As a consequence, the associated computational complexity for implementation is reduced. Moreover, the state estimate of the DQ-MEKF can be directly used by the pose controllers given in Refs. [7, 8] without additional conversions.
3) Similarly to the Q-MEKF, the DQ-MEKF is a *continuous-discrete Kalman filter*,[16] i.e., the state and its covariance matrix are propagated continuously between discrete-time measurements. One of the advantages of this approach is that the discrete-time measurements do not need to be equally spaced in time, making irregular or intermittent measurements easy to handle. Moreover, this structure eases the incorporation of different sensors with different update rates. In particular, the DQ-MEKF described in this paper is designed to take continuous-time linear and angular velocity measurements with noise and bias and discrete-time pose measurements with noise. This

paper also proposes two extensions of this standard DQ-MEKF. The first extension is designed to take only discrete-time pose measurements with noise and estimate the linear and angular velocities. This version is suitable for satellite proximity operation scenarios where the chaser satellite has only access to measurements of the relative pose (e.g., from a camera), but requires the relative linear and angular velocities for control. In the second extension, the linear velocity measurements of the standard DQ-MEKF are replaced with linear acceleration measurements with bias and noise. This version is suitable for a satellite equipped with an accelerometer and having no means of directly measuring linear velocity.

4) Finally, the two extensions of the standard DQ-MEKF are validated experimentally on a 5-DOF air-bearing platform. The first extension is also compared with two alternative EKF formulations, similar to the ones used in Refs. [10–13], on the same 5-DOF platform and through Monte-Carlo simulations. It is shown that the DQ-MEKF compares favorably with these alternative formulations.

This paper is organized as follows. In Section II the main equations of a standard EKF are reviewed. Then, the DQ-MEKF is derived in Section III, starting with a brief introduction about quaternions and dual quaternions and ending with the derivation of two variations of the DQ-MEKF that may be most useful for spacecraft proximity operations in space. In Section IV the DQ-MEKF is validated experimentally and compared with two alternative EKF formulations. Finally, in Section V the first extension is compared again with the same two alternative EKF formulations through Monte-Carlo simulations.

II. The Extended Kalman Filter

The main equations of the EKF are reviewed in order to introduce the necessary notation for the remaining sections. The review is based on a similar review provided in Ref. [1] and serves as the starting point of the DQ-MEKF formulation.

The state equation of the EKF can be written as

$$\dot{x}_n(t) = f_n(x_n(t), t) + g_{n\times p}(x_n(t), t)w_p(t), \tag{1}$$

where $x_n(t) \in \mathbb{R}^n$ is the state and $w_p(t) \in \mathbb{R}^p$ is the process noise. The process noise is assumed to be a Gaussian white-noise process, whose mean and covariance are given by $E\{w_p(t)\} = 0_{p\times 1}$ and $E\left\{w_p(t)w_p^\intercal(\tau)\right\} = Q_{p\times p}(t)\delta(t-\tau)$, respectively, where $Q_{p\times p}(t) \in \mathbb{R}^{p\times p}$ is a symmetric positive semidefinite matrix. The initial mean and covariance of the state are given by $E\{x_n(t_0)\} \triangleq \hat{x}_n(t_0) = x_{n,0} \in \mathbb{R}^n$ and $E\{(x_n(t_0) - x_{n,0})(x_n(t_0) - x_{n,0})^\intercal\} \triangleq P_{n\times n}(t_0) = P_{n\times n,0} \in \mathbb{R}^{n\times n}$ and are assumed to be known. (Note that in Refs. [14, 15], $p = n$

and $g_{n\times p}(x_n(t),t) = I_{n\times n}$.)

II.A. Time Update

Given the initial mean of the state, the minimum covariance estimate of the state at a future time t in the absence of measurements is given by the conditional expectation $\hat{x}_n(t) = E\{x_n(t)|\hat{x}_n(t_0) = x_{n,0}\}$. This estimate satisfies the differential equation $\dot{\hat{x}}_n(t) = E\{f_n(x_n(t),t)\}$, which is typically approximated as

$$\dot{\hat{x}}_n(t) \approx f_n(\hat{x}_n(t),t). \tag{2}$$

Hence, in the absence of measurements, the state estimate is propagated using Eq. (2).

In addition to the state estimate, also the covariance matrix of the state needs to be propagated. The covariance matrix of the state is given by $P_{n\times n}(t) = E\{\Delta x_n(t)\Delta x_n^{\mathsf{T}}(t)\} \in \mathbb{R}^{n\times n}$, where $\Delta x_n(t) = x_n(t) - \hat{x}_n(t) \in \mathbb{R}^n$ is the state error. As a first-order approximation, the derivative of the state error is given by

$$\frac{\mathrm{d}}{\mathrm{d}t}\Delta x_n(t) = F_{n\times n}(t)\Delta x_n(t) + G_{n\times p}(t)w_p(t), \tag{3}$$

and the covariance matrix of the state satisfies the Riccati equation

$$\dot{P}_{n\times n}(t) = F_{n\times n}(t)P_{n\times n}(t) + P_{n\times n}(t)F_{n\times n}^{\mathsf{T}}(t) + G_{n\times p}(t)Q_{p\times p}(t)G_{n\times p}^{\mathsf{T}}(t), \tag{4}$$

where

$$F_{n\times n}(t) \triangleq \left.\frac{\partial f_n(x_n,t)}{\partial x_n}\right|_{\hat{x}_n(t)} \in \mathbb{R}^{n\times n} \quad \text{and} \quad G_{n\times p}(t) \triangleq g_{n\times p}(\hat{x}_n(t),t) \in \mathbb{R}^{n\times p} \tag{5}$$

Hence, in the absence of measurements, the covariance matrix of the state is propagated using Eq. (4)-(5).

II.B. Measurement Update

Assume that a measurement is taken at time t_k that is related with the state of the EKF through the nonlinear output equation

$$z_m(t_k) = h_m(x_n(t_k)) + v_m(t_k) \in \mathbb{R}^m, \tag{6}$$

where $v_m(t_k) \in \mathbb{R}^m$ is the measurement noise assumed to be a discrete Gaussian white-noise process, whose mean and covariance are given by $E\{v_m(t_k)\} = 0_{m\times 1}$ and $E\{v_m(t_k)v_m^{\mathsf{T}}(t_\ell)\} = R_{m\times m}(t_k)\delta_{t_k t_\ell}$, where $R_{m\times m}(t_k) \in \mathbb{R}^{m\times m}$ is a symmetric positive definite matrix.

Immediately following the measurement at time t_k, the minimum variance estimate of $x_n(t_k)$ is given by

$$\hat{x}_n^+(t_k) = \hat{x}_n^-(t_k) + \Delta^\star \hat{x}_n(t_k), \tag{7}$$

where

$$\Delta^\star \hat{x}_n(t_k) = K_{n\times m}(t_k)[z_m(t_k) - \hat{z}_m(t_k)] \tag{8}$$

is the optimal Kalman state update, where

$$\hat{z}_m(t_k) = h_m(\hat{x}_n^-(t_k)), \tag{9}$$

and $\hat{x}_n^-(t_k)$ and $\hat{x}_n^+(t_k)$ are the predicted values of the state immediately before and after the measurement, and $K_{n\times m}(t_k)$ is the Kalman gain. The Kalman gain is given by

$$K_{n\times m}(t_k) = P_{n\times n}^-(t_k)H_{m\times n}^\mathsf{T}(t_k)[H_{m\times n}(t_k)P_{n\times n}^-(t_k)H_{m\times n}^\mathsf{T}(t_k) + R_{m\times m}(t_k)]^{-1}, \tag{10}$$

where $P_{n\times n}^-(t_k)$ is the predicted state covariance matrix immediately before the measurement and

$$H_{m\times n}(t_k) = \left.\frac{\partial h_m(x_n)}{\partial x_n}\right|_{\hat{x}_n^-(t_k)} \in \mathbb{R}^{m\times n} \tag{11}$$

is the measurement sensitivity matrix.

Immediately after the measurement, the state covariance matrix is given by

$$\begin{aligned} P_{n\times n}^+(t_k) &= (I_{n\times n} - K_{n\times m}(t_k)H_{m\times n}(t_k))P_{n\times n}^-(t_k) &(12)\\ &= (I_{n\times n} - K_{n\times m}(t_k)H_{m\times n}(t_k))P_{n\times n}^-(t_k)(I_{n\times n} - K_{n\times m}(t_k)H_{m\times n}(t_k))^\mathsf{T} \\ &+ K_{n\times m}(t_k)R_{m\times m}(t_k)K_{n\times m}(t_k)^\mathsf{T}, &(13)\end{aligned}$$

where Eq. (13) is numerically more stable than Eq. (12).

III. Extended Kalman Filter for Spacecraft Pose Estimation Using Dual Quaternions

This section provides a quick introduction to quaternions and dual quaternions. Then, a combined angular and linear velocity measurement model analogous to the angular velocity measurement model described in Ref. [1] is proposed. After that, the DQ-MEKF for pose estimation based on dual quaternions is derived using dual quaternion algebra. Finally, two versions of the DQ-MEKF that may be useful in practice are proposed. The first one is useful when angular and linear velocity measurements are not available, i.e., only pose measurements are available, and the second is useful when linear velocity measurements are

replaced by linear acceleration measurements.

III.A. Mathematical Preliminaries

For the benefit of the reader, the main properties of quaternions and dual quaternions, which are essential for deriving the results presented in this paper, are summarized in this section. For additional information on quaternions and dual quaternions, the reader is referred to Refs. [7, 17].

III.A.1. Quaternions

A quaternion is defined as $q = q_0 + q_1 i + q_2 j + q_3 k$, where q_0, q_1, q_2, $q_3 \in \mathbb{R}$ and i, j, and k satisfy $i^2 = j^2 = k^2 = -1$, $i = jk = -kj$, $j = ki = -ik$, and $k = ij = -ji$.[18] A quaternion can also be represented as the ordered pair $q = (q_0, \overline{q})$, where $\overline{q} = [q_1 \; q_2 \; q_3]^\intercal \in \mathbb{R}^3$ is the *vector part* of the quaternion and $q_0 \in \mathbb{R}$ is the *scalar part* of the quaternion. *Vector quaternions* and *scalar quaternions* are quaternions with zero scalar part and vector part, respectively. The set of quaternions, vector quaternions, and scalar quaternions will be denoted by $\mathbb{H} = \{q : \; q = q_0 + q_1 i + q_2 j + q_3 k, \; q_0, q_1, q_2, q_3 \in \mathbb{R}\}$, $\mathbb{H}^v = \{q \in \mathbb{H} : \; q_0 = 0\}$, and $\mathbb{H}^s = \{q \in \mathbb{H} : \; q_1 = q_2 = q_3 = 0\}$, respectively.

The basic operations between quaternions are defined as follows:

$$\begin{gathered}
\text{Addition: } a + b = (a_0 + b_0, \overline{a} + \overline{b}) \in \mathbb{H}, \\
\text{Multiplication by a scalar: } \lambda a = (\lambda a_0, \lambda \overline{a}) \in \mathbb{H}, \\
\text{Multiplication: } ab = (a_0 b_0 - \overline{a} \cdot \overline{b}, a_0 \overline{b} + b_0 \overline{a} + \overline{a} \times \overline{b}) \in \mathbb{H}, \\
\text{Conjugation: } a^* = (a_0, -\overline{a}) \in \mathbb{H}, \\
\text{Dot product: } a \cdot b = \tfrac{1}{2}(a^* b + b^* a) = \tfrac{1}{2}(a b^* + b a^*) = (a_0 b_0 + \overline{a} \cdot \overline{b}, 0_{3\times 1}) \in \mathbb{H}^s, \\
\text{Cross product: } a \times b = \tfrac{1}{2}(ab - b^* a^*) = (0, b_0 \overline{a} + a_0 \overline{b} + \overline{a} \times \overline{b}) \in \mathbb{H}^v,
\end{gathered} \tag{14}$$

where $a, b \in \mathbb{H}$, $\lambda \in \mathbb{R}$, and $0_{m\times n}$ is a m-by-n matrix of zeros. Note that the quaternion multiplication is not commutative. In fact, some authors[1] define Eq. (14) as ba, and not as ab as originally defined by Hamilton.[19] This paper follows the original definition by Hamilton. Finally, the quaternions $(1, \bar{0})$ and $(0, \bar{0})$ will be denoted by $\mathtt{1}$ and $\mathtt{0}$, respectively.

The bijective mapping between the set of quaternions and $\mathbb{R}^4$ will be denoted by $[\,\cdot\,] : \mathbb{H} \to \mathbb{R}^4$, where $[q] = [q_0 \; q_1 \; q_2 \; q_3]^\intercal$. Using this mapping, the cross product of $a \in \mathbb{H}^v$ with

$b \in \mathbb{H}^v$ can be computed as $[a \times b] = [a]^\times [b]$, where $[\,\cdot\,]^\times : \mathbb{H}^v \to \mathbb{R}^{4\times 4}$ is defined as

$$[a]^\times = \begin{bmatrix} 0 & 0_{1\times 3} \\ 0_{3\times 1} & \overline{a}^\times \end{bmatrix}, \quad \text{where} \quad \overline{a}^\times = \begin{bmatrix} 0 & -a_3 & a_2 \\ a_3 & 0 & -a_1 \\ -a_2 & a_1 & 0 \end{bmatrix}. \tag{15}$$

Likewise, the left quaternion multiplication of $a \in \mathbb{H}$ with $b \in \mathbb{H}$ can be computed as $[ab] = [\![a]\!][b]$, where $[\![\,\cdot\,]\!] : \mathbb{H} \to \mathbb{R}^{4\times 4}$ is defined as

$$[\![a]\!] = \begin{bmatrix} a_0 & -\overline{a}^\intercal \\ \overline{a} & [\widetilde{a}] \end{bmatrix}, \quad \text{where} \quad [\widetilde{a}] = a_0 I_{3\times 3} + \overline{a}^\times. \tag{16}$$

The relative orientation of a frame fixed to a body with respect to another frame, denoted here as the I-frame, can be represented by the *unit* quaternion $q_{\text{B/I}} = \big(\cos(\frac{\phi}{2}), \sin(\frac{\phi}{2})\bar{n}\big)$, where the body frame is said to be rotated with respect to the I-frame about the unit vector $\bar{n}$ by an angle ϕ. A unit quaternion is defined as a quaternion that belongs to the set $\mathbb{H}^u = \{q \in \mathbb{H} : \; q \cdot q = qq^* = q^*q = 1\}$. From this constraint, assuming that $-180 < \phi < 180$ deg, the scalar part of a unit quaternion can be computed from

$$q_0 = \sqrt{1 - \|\overline{q}\|^2}, \tag{17}$$

where $\|\cdot\|$ denotes the usual Euclidean norm in $\mathbb{R}^3$.

The coordinates of a vector in the B-frame, $\overline{v}^{\text{B}}$, can be calculated from the coordinates of the same vector in the I-frame, $\overline{v}^{\text{I}}$, and vice-versa, via $v^{\text{B}} = q^*_{\text{B/I}} v^{\text{I}} q_{\text{B/I}}$ and $v^{\text{I}} = q_{\text{B/I}} v^{\text{B}} q^*_{\text{B/I}}$, where $v^{\text{B}} = (0, \overline{v}^{\text{B}})$ and $v^{\text{I}} = (0, \overline{v}^{\text{I}})$. This is equivalent to $\overline{v}^{\text{B}} = R(q_{\text{B/I}})\overline{v}^{\text{I}}$ and $\overline{v}^{\text{I}} = R(q^*_{\text{B/I}})\overline{v}^{\text{B}}$, where $R(q_{\text{B/I}})$ and $R(q^*_{\text{B/I}})$ are the rotation matrices corresponding to $q_{\text{B/I}}$ and $q^*_{\text{B/I}}$, respectively.

III.A.2. Dual Quaternions

A dual quaternion is defined as $\boldsymbol{q} = q_r + \epsilon q_d$, where ϵ is the *dual unit* defined by $\epsilon^2 = 0$ and $\epsilon \neq 0$. The quaternions $q_r, q_d \in \mathbb{H}$ are the *real part* and the *dual part* of the dual quaternion, respectively. *Dual vector quaternions* and *dual scalar quaternions* are dual quaternions formed from vector quaternions (i.e., $q_r, q_d \in \mathbb{H}^v$) and scalar quaternions (i.e., $q_r, q_d \in \mathbb{H}^s$), respectively. The set of dual quaternions, dual scalar quaternions, and dual vector quaternions will be denoted by $\mathbb{H}_d = \{\boldsymbol{q} : \; \boldsymbol{q} = q_r + \epsilon q_d, \; q_r, q_d \in \mathbb{H}\}$, $\mathbb{H}^s_d = \{\boldsymbol{q} : \; \boldsymbol{q} = q_r + \epsilon q_d, \; q_r, q_d \in \mathbb{H}^s\}$, and $\mathbb{H}^v_d = \{\boldsymbol{q} : \; \boldsymbol{q} = q_r + \epsilon q_d, \; q_r, q_d \in \mathbb{H}^v\}$, respectively.

The basic operations between dual quaternions are defined as follows:[20,21]

$$\text{Addition: } \boldsymbol{a}+\boldsymbol{b}=(a_r+b_r)+\epsilon(a_d+b_d)\in\mathbb{H}_d,$$
$$\text{Multiplication by a scalar: } \lambda\boldsymbol{a}=(\lambda a_r)+\epsilon(\lambda a_d)\in\mathbb{H}_d,$$
$$\text{Multiplication: } \boldsymbol{a}\boldsymbol{b}=(a_r b_r)+\epsilon(a_r b_d+a_d b_r)\in\mathbb{H}_d,$$
$$\text{Conjugation: } \boldsymbol{a}^*=a_r^*+\epsilon a_d^*\in\mathbb{H}_d,$$
$$\text{Dot product: } \boldsymbol{a}\cdot\boldsymbol{b}=\tfrac{1}{2}(\boldsymbol{a}^*\boldsymbol{b}+\boldsymbol{b}^*\boldsymbol{a})=\tfrac{1}{2}(\boldsymbol{a}\boldsymbol{b}^*+\boldsymbol{b}\boldsymbol{a}^*)=a_r\cdot b_r+\epsilon(a_d\cdot b_r+a_r\cdot b_d)\in\mathbb{H}_d^s,$$
$$\text{Cross product: } \boldsymbol{a}\times\boldsymbol{b}=\tfrac{1}{2}(\boldsymbol{a}\boldsymbol{b}-\boldsymbol{b}^*\boldsymbol{a}^*)=a_r\times b_r+\epsilon(a_d\times b_r+a_r\times b_d)\in\mathbb{H}_d^v,$$

where $\boldsymbol{a},\boldsymbol{b}\in\mathbb{H}_d$ and $\lambda\in\mathbb{R}$. Note that the dual quaternion multiplication is not commutative. In this paper, the dual quaternions $1+\epsilon 0$ and $0+\epsilon 0$ will be denoted by $\mathbf{1}$ and $\mathbf{0}$, respectively.

The bijective mapping between the set of dual quaternions and $\mathbb{R}^8$ will be denoted by $[\,\cdot\,]:\mathbb{H}_d\to\mathbb{R}^8$, where $[\boldsymbol{q}]=[[q_r]^\mathsf{T}[q_d]^\mathsf{T}]^\mathsf{T}$. Using this mapping, the left dual quaternion multiplication of $\boldsymbol{a}\in\mathbb{H}_d$ with $\boldsymbol{b}\in\mathbb{H}_d$ can be computed as $[\boldsymbol{a}\boldsymbol{b}]=[\![\boldsymbol{a}]\!][\boldsymbol{b}]$, where $[\![\,\cdot\,]\!]:\mathbb{H}_d\to\mathbb{R}^{8\times 8}$ is defined as

$$[\![\boldsymbol{a}]\!]=\begin{bmatrix}[\![a_r]\!] & 0_{4\times 4}\\ [\![a_d]\!] & [\![a_r]\!]\end{bmatrix}. \tag{18}$$

Finally, it is convenient to define $[\widetilde{\cdot}]:\mathbb{H}_d\to\mathbb{R}^{6\times 6}$ as

$$[\widetilde{\boldsymbol{a}}]=\begin{bmatrix}[\widetilde{a}_r] & 0_{3\times 3}\\ [\widetilde{a}_d] & [\widetilde{a}_r]\end{bmatrix}, \tag{19}$$

where $\overline{\cdot}:\mathbb{H}_d\to\mathbb{R}^6$ is defined as $\overline{\boldsymbol{a}}=[\overline{a_r}^\mathsf{T}\ \overline{a_d}^\mathsf{T}]^\mathsf{T}\in\mathbb{R}^6$, and $\overline{\cdot}^\times:\mathbb{H}_d\to\mathbb{R}^{6\times 6}$ is defined as

$$\overline{\boldsymbol{a}}^\times=\begin{bmatrix}\overline{a}_r^\times & 0_{3\times 3}\\ \overline{a}_d^\times & \overline{a}_r^\times\end{bmatrix}. \tag{20}$$

Similarly, $(\,\cdot\,)_r:\mathbb{H}_d\to\mathbb{H}$ is defined as $(\boldsymbol{a})_r=a_r$ and $(\,\cdot\,)_d:\mathbb{H}_d\to\mathbb{H}$ is defined as $(\boldsymbol{a})_d=a_d$.

The attitude and position (i.e., pose) of a body frame with respect to another frame, say, the I-frame, can be represented by a *unit* quaternion $q_{\mathrm{B/I}}\in\mathbb{H}^u$ and by a translation vector $\overline{r}^{\mathrm{I}}_{\mathrm{B/I}}\in\mathbb{R}^3$ or $\overline{r}^{\mathrm{B}}_{\mathrm{B/I}}\in\mathbb{R}^3$, where $\overline{r}^{\mathrm{X}}_{\mathrm{Y/Z}}$ is the translation vector from the origin of the Z-frame to the origin of the Y-frame expressed in the X-frame. Alternatively, the pose of the body frame with respect to another frame can be represented more compactly by the *unit* dual quaternion[22]

$$\boldsymbol{q}_{\mathrm{B/I}}=q_{\mathrm{B/I},r}+\epsilon q_{\mathrm{B/I},d}=q_{\mathrm{B/I}}+\epsilon\tfrac{1}{2}r^{\mathrm{I}}_{\mathrm{B/I}}q_{\mathrm{B/I}}=q_{\mathrm{B/I}}+\epsilon\tfrac{1}{2}q_{\mathrm{B/I}}r^{\mathrm{B}}_{\mathrm{B/I}}, \tag{21}$$

where $r^{\mathrm{X}}_{\mathrm{Y/Z}}=(0,\overline{r}^{\mathrm{X}}_{\mathrm{Y/Z}})$. Note that the dual part of $\boldsymbol{q}_{\mathrm{B/I}}$, i.e., $q_{\mathrm{B/I},d}$, is a representation of

the position of the body frame with respect to the I-frame. Given $\boldsymbol{q}_{\mathrm{B/I}}$, the position of the body frame with respect to the I-frame can be obtained in I-frame coordinates from $r^{\mathrm{I}}_{\mathrm{B/I}} = 2q_{\mathrm{B/I},d}q^{*}_{\mathrm{B/I}}$ and in B-frame coordinates from $r^{\mathrm{B}}_{\mathrm{B/I}} = 2q^{*}_{\mathrm{B/I}}q_{\mathrm{B/I},d}$. Figure 1 illustrates this relation between $r^{\mathrm{B}}_{\mathrm{B/I}}$, $q_{\mathrm{B/I},d}$, and $r^{\mathrm{I}}_{\mathrm{B/I}}$. Note that whereas the relation between $r^{\mathrm{B}}_{\mathrm{B/I}}$ and $r^{\mathrm{I}}_{\mathrm{B/I}}$ is quadratic in $q_{\mathrm{B/I}}$, $q_{\mathrm{B/I},d}$ is related linearly in $q_{\mathrm{B/I}}$ with $r^{\mathrm{B}}_{\mathrm{B/I}}$ and $r^{\mathrm{I}}_{\mathrm{B/I}}$.

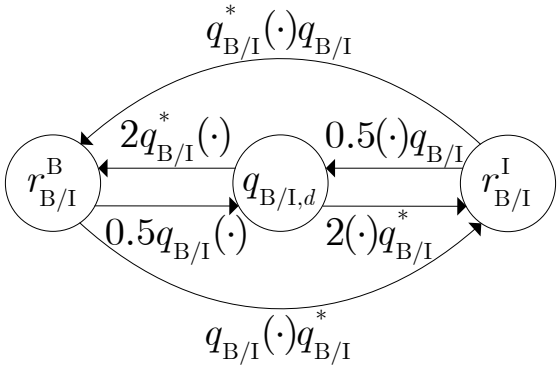

Figure 1. Relation between $r^{\mathrm{B}}_{\mathrm{B/I}}$, $q_{\mathrm{B/I},d}$, and $r^{\mathrm{I}}_{\mathrm{B/I}}$.

A *unit* dual quaternion is defined as a dual quaternion that belongs to the set[23]

$$\mathbb{H}^{u}_{d} = \{\boldsymbol{q} \in \mathbb{H}_{d} : \ \boldsymbol{q}\cdot\boldsymbol{q} = \boldsymbol{q}\boldsymbol{q}^{*} = \boldsymbol{q}^{*}\boldsymbol{q} = \mathbf{1}\} = \{\boldsymbol{q} \in \mathbb{H}_{d} : \ q_r \cdot q_r = \mathtt{1} \text{ and } q_r \cdot q_d = \mathtt{0}\}. \tag{22}$$

From this constraint, assuming that $-180 < \phi < 180$ deg, the scalar parts of the real and dual parts of a unit dual quaternion can be computed from their respective vector parts from

$$q_{r,0} = \sqrt{1 - \|\overline{q}_r\|^2} \quad \text{and} \quad q_{d,0} = \frac{-\overline{q_r}^{\mathsf{T}}\overline{q_d}}{q_{r,0}}. \tag{23}$$

The rotational and translational kinematic equations of the body frame with respect to another frame can be written compactly in terms of dual quaternions as[22]

$$\dot{\boldsymbol{q}}_{\mathrm{B/I}} = \tfrac{1}{2}\boldsymbol{\omega}^{\mathrm{I}}_{\mathrm{B/I}}\boldsymbol{q}_{\mathrm{B/I}} = \tfrac{1}{2}\boldsymbol{q}_{\mathrm{B/I}}\boldsymbol{\omega}^{\mathrm{B}}_{\mathrm{B/I}}, \tag{24}$$

where $\boldsymbol{\omega}^{\mathrm{X}}_{\mathrm{Y/Z}}$ is the *dual velocity* of the Y-frame with respect to the Z-frame expressed in the X-frame, $\boldsymbol{\omega}^{\mathrm{B}}_{\mathrm{B/I}} \triangleq \omega^{\mathrm{B}}_{\mathrm{B/I}} + \epsilon v^{\mathrm{B}}_{\mathrm{B/I}}$, $\boldsymbol{\omega}^{\mathrm{I}}_{\mathrm{B/I}} \triangleq \omega^{\mathrm{I}}_{\mathrm{B/I}} + \epsilon(v^{\mathrm{I}}_{\mathrm{B/I}} - \omega^{\mathrm{I}}_{\mathrm{B/I}} \times r^{\mathrm{I}}_{\mathrm{B/I}})$, $\omega^{\mathrm{X}}_{\mathrm{Y/Z}} = (0, \overline{\omega}^{\mathrm{X}}_{\mathrm{Y/Z}})$, $\overline{\omega}^{\mathrm{X}}_{\mathrm{Y/Z}}$ is the angular velocity of the Y-frame with respect to the Z-frame expressed in the X-frame, $v^{\mathrm{X}}_{\mathrm{Y/Z}} = (0, \overline{v}^{\mathrm{X}}_{\mathrm{Y/Z}})$, and $\overline{v}^{\mathrm{X}}_{\mathrm{Y/Z}}$ is the linear velocity of the origin of the Y-frame with respect to the Z-frame expressed in the X-frame. Note that the rotational and translational kinematic equations written in terms of dual quaternions have the same form as the rotational-only kinematic equations written in terms of quaternions.[7]

III.B. Angular and Linear Velocity Measurement Model

The dual velocity measurement model is defined analogously to the angular velocity measurement model typically used in literature,[1,2] i.e.,

$$\boldsymbol{\omega}^{\mathrm{B}}_{\mathrm{B/I},m} = \boldsymbol{\omega}^{\mathrm{B}}_{\mathrm{B/I}} + \boldsymbol{b}_{\boldsymbol{\omega}} + \boldsymbol{\eta}_{\boldsymbol{\omega}}, \tag{25}$$

where $\boldsymbol{\omega}^{\mathrm{B}}_{\mathrm{B/I},m} = \omega^{\mathrm{B}}_{\mathrm{B/I},m} + \epsilon v^{\mathrm{B}}_{\mathrm{B/I},m} \in \mathbb{H}^v_d$, $\omega^{\mathrm{B}}_{\mathrm{B/I},m} = (0, \overline{\omega}^{\mathrm{B}}_{\mathrm{B/I},m})$, $\overline{\omega}^{\mathrm{B}}_{\mathrm{B/I},m}$ is a measurement of the angular velocity of the body frame with respect to the I-frame expressed in the body frame, $v^{\mathrm{B}}_{\mathrm{B/I},m} = (0, \overline{v}^{\mathrm{B}}_{\mathrm{B/I},m})$, $\overline{v}^{\mathrm{B}}_{\mathrm{B/I},m}$ is a measurement of the linear velocity of the origin of the body frame with respect to the I-frame expressed in the body frame, $\boldsymbol{b}_{\boldsymbol{\omega}} = b_\omega + \epsilon b_v$ is the dual bias, $b_\omega = (0, \overline{b}_\omega)$, $\overline{b}_\omega \in \mathbb{R}^3$ is the bias of the angular velocity measurement, $b_v = (0, \overline{b}_v)$, $\overline{b}_v \in \mathbb{R}^3$ is the bias of the linear velocity measurement, $\boldsymbol{\eta}_{\boldsymbol{\omega}} = \eta_\omega + \epsilon \eta_v$, $\eta_\omega = (0, \overline{\eta}_\omega)$, $\overline{\eta}_\omega \in \mathbb{R}^3$ is the noise of the angular velocity measurement assumed to be a zero-mean Gaussian white noise process, $\eta_v = (0, \overline{\eta}_v)$, and $\overline{\eta}_v \in \mathbb{R}^3$ is the noise of the linear velocity measurement assumed to be a Gaussian white-noise process with $E\{\overline{\boldsymbol{\eta}}_{\boldsymbol{\omega}}\} = 0_{6\times 1}$, and covariance

$$E\{\overline{\boldsymbol{\eta}}_{\boldsymbol{\omega}}(t)\overline{\boldsymbol{\eta}}^{\mathrm{T}}_{\boldsymbol{\omega}}(\tau)\} = \overline{Q}_{\boldsymbol{\omega}}(t)\delta(t-\tau) = \begin{bmatrix} \overline{Q}_\omega(t) & \overline{Q}_{\omega v}(t) \\ \overline{Q}_{\omega v}(t) & \overline{Q}_v(t) \end{bmatrix} \delta(t-\tau), \tag{26}$$

where $\overline{Q}_{\boldsymbol{\omega}}(t) \in \mathbb{R}^{6\times 6}$ is a symmetric positive semidefinite matrix. The dual bias is not constant, but assumed to be driven by another zero-mean Gaussian white noise process through

$$\dot{\boldsymbol{b}}_{\boldsymbol{\omega}} = \boldsymbol{\eta}_{\boldsymbol{b\omega}}, \tag{27}$$

where $\boldsymbol{\eta}_{\boldsymbol{b\omega}} = (0, \overline{\eta}_{b_\omega}) + \epsilon(0, \overline{\eta}_{b_v})$, $E\left\{\overline{\boldsymbol{\eta}}_{\boldsymbol{b\omega}}\right\} = 0_{6\times 1}$, and covariance

$$E\left\{\overline{\boldsymbol{\eta}}_{\boldsymbol{b\omega}}(t)\overline{\boldsymbol{\eta}}^{\mathrm{T}}_{\boldsymbol{b\omega}}(\tau)\right\} = \overline{Q}_{\boldsymbol{b\omega}}(t)\delta(t-\tau) = \begin{bmatrix} \overline{Q}_{b_\omega}(t) & \overline{Q}_{b_\omega b_v}(t) \\ \overline{Q}_{b_\omega b_v}(t) & \overline{Q}_{b_v}(t) \end{bmatrix} \delta(t-\tau), \tag{28}$$

where $\overline{Q}_{\boldsymbol{b\omega}}(t) \in \mathbb{R}^{6\times 6}$ is a symmetric positive semidefinite matrix.

If the I-frame is inertial, $\boldsymbol{\omega}^{\mathrm{B}}_{\mathrm{B/I}}$ should be interpreted as the inertial angular and linear velocities of the satellite expressed in the B-frame. In that case, $\boldsymbol{\omega}^{\mathrm{B}}_{\mathrm{B/I}}$ can be measured using a combination of, say, rate-gyros, Doppler radar, and GPS. On the other hand, if the I-frame is not inertial, $\boldsymbol{\omega}^{\mathrm{B}}_{\mathrm{B/I}}$ should be interpreted as the relative angular and linear velocities of the satellite with respect to a frame attached, for example, to another satellite. In that case, $\boldsymbol{\omega}^{\mathrm{B}}_{\mathrm{B/I}}$ can be measured using a combination of, say, rate-gyros on both satellites,[12] Doppler radar, differential GPS, and LIDAR.

III.C. Dual Quaternion Multiplicative Extended Kalman Filter (DQ-MEFK)

In this section, the DQ-MEKF for pose estimation is derived. The state and process noise of the DQ-MEKF are initially selected as

$$x_{16} = \begin{bmatrix} [\delta \boldsymbol{q}_{\mathrm{B/I}}] \\ [\boldsymbol{b}_{\boldsymbol{\omega}}] \end{bmatrix} \in \mathbb{R}^{16} \quad \text{and} \quad w_{16} = \begin{bmatrix} [\boldsymbol{\eta}_{\boldsymbol{\omega}}] \\ [\boldsymbol{\eta}_{\boldsymbol{b}_{\boldsymbol{\omega}}}] \end{bmatrix} \in \mathbb{R}^{16}, \tag{29}$$

where the dual error quaternion $\delta \boldsymbol{q}_{\mathrm{B/I}} \in \mathbb{H}_d^u$ is defined analogously to the error quaternion[1] $\delta q_{\mathrm{B/I}} = \hat{q}^*_{\mathrm{B/I}} q_{\mathrm{B/I}} \in \mathbb{H}^u$ as

$$\delta \boldsymbol{q}_{\mathrm{B/I}} = \hat{\boldsymbol{q}}^*_{\mathrm{B/I}} \boldsymbol{q}_{\mathrm{B/I}} \in \mathbb{H}_d^u, \tag{30}$$

i.e., $\delta \boldsymbol{q}_{\mathrm{B/I}} \in \mathbb{H}_d^u$ is the dual quaternion between the actual dual quaternion $\boldsymbol{q}_{\mathrm{B/I}} \in \mathbb{H}_d^u$ and its current best guess $\hat{\boldsymbol{q}}_{\mathrm{B/I}} \in \mathbb{H}_d^u$. Analogously to the propagation of $\hat{q}_{\mathrm{B/I}} \in \mathbb{H}^u$ in Ref. [4], $\hat{\boldsymbol{q}}_{\mathrm{B/I}}$ is propagated using

$$\frac{\mathrm{d}}{\mathrm{d}t}(\hat{\boldsymbol{q}}_{\mathrm{B/I}}) \approx \tfrac{1}{2} \hat{\boldsymbol{q}}_{\mathrm{B/I}} \hat{\boldsymbol{\omega}}^{\mathrm{B}}_{\mathrm{B/I}}, \tag{31}$$

where, from Eq. (25),

$$\hat{\boldsymbol{\omega}}^{\mathrm{B}}_{\mathrm{B/I}} \triangleq E\left\{\boldsymbol{\omega}^{\mathrm{B}}_{\mathrm{B/I}}\right\} = E\left\{\boldsymbol{\omega}^{\mathrm{B}}_{\mathrm{B/I},m} - \boldsymbol{b}_{\boldsymbol{\omega}} - \boldsymbol{\eta}_{\boldsymbol{\omega}}\right\} = \boldsymbol{\omega}^{\mathrm{B}}_{\mathrm{B/I},m} - \hat{\boldsymbol{b}}_{\boldsymbol{\omega}}, \tag{32}$$

with $\hat{\boldsymbol{b}}_{\boldsymbol{\omega}} \triangleq E\left\{\boldsymbol{b}_{\boldsymbol{\omega}}\right\}$ and

$$\frac{\mathrm{d}}{\mathrm{d}t}\left(\hat{\boldsymbol{b}}_{\boldsymbol{\omega}}\right) = E\left\{\boldsymbol{\eta}_{\boldsymbol{b}_{\boldsymbol{\omega}}}\right\} = \mathbf{0}. \tag{33}$$

The approximation in Eq. (31) is a result of using the typical EKF approximation given by Eq. (2) in the derivation of Eq. (31).[4]

Analogously to Ref. [4], for $-180 < \phi < 180$ deg, $\delta \boldsymbol{q}_{\mathrm{B/I}}$ is parameterized by $\overline{\delta \boldsymbol{q}_{\mathrm{B/I}}}$ and the expected value of $\overline{\delta \boldsymbol{q}_{\mathrm{B/I}}}$ is required to be zero, i.e., $E\left\{\overline{\delta \boldsymbol{q}_{\mathrm{B/I}}}\right\} = 0_{6\times 1}$. Hence, $E\left\{\delta \boldsymbol{q}_{\mathrm{B/I}}\left(\overline{\delta \boldsymbol{q}_{\mathrm{B/I}}}\right)\right\} = \mathbf{1}$.

Note that the current best guess of $\boldsymbol{q}_{\mathrm{B/I}}$, given by $\hat{\boldsymbol{q}}_{\mathrm{B/I}}$, is not defined as the standard expected value of the random variable $\boldsymbol{q}_{\mathrm{B/I}}$ as this would require the expectation to be defined with respect to a non-trivial probability density function in $\mathbb{H}_d^u$. As shown in Ref. [5], even the definition of probability density function on $\mathbb{H}^u$ is not trivial. A complete discussion of probability density functions in $\mathbb{H}_d^u$ is outside the scope of this paper. The reader is referred to Ref. [5] for a discussion of possible probability density functions in $\mathbb{H}^u$.

A geometric interpretation of the dual error quaternion $\delta \boldsymbol{q}_{\mathrm{B/I}}$ is given in Fig. 2. It is the dual unit quaternion that describes the relative pose between the B-frame and the $\hat{\mathrm{B}}$-frame. The B-frame represents the true pose of the body-frame, whereas the $\hat{\mathrm{B}}$-frame represents the expected pose of the body-frame, in other words, it represents the best available guess of the

pose of the body-frame.

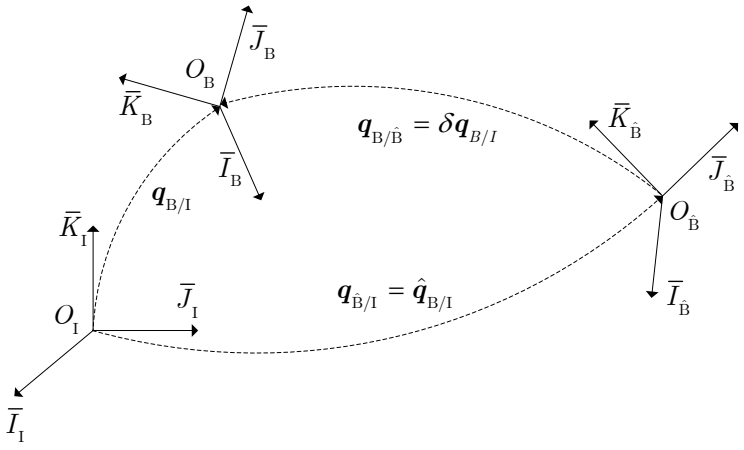

Figure 2. Interpretation of the dual error quaternion.

To determine the state equation of the DQ-MEKF, the time derivative of $\delta\boldsymbol{q}_{\mathrm{B/I}}$ needs to be calculated. Taking the time derivative of Eq. (30) yields

$$\frac{\mathrm{d}}{\mathrm{d}t}(\delta\boldsymbol{q}_{\mathrm{B/I}}) = \frac{\mathrm{d}}{\mathrm{d}t}(\hat{\boldsymbol{q}}^{*}_{\mathrm{B/I}})\boldsymbol{q}_{\mathrm{B/I}} + \hat{\boldsymbol{q}}^{*}_{\mathrm{B/I}}\frac{\mathrm{d}}{\mathrm{d}t}(\boldsymbol{q}_{\mathrm{B/I}}). \tag{34}$$

Substituting Eqs. (24) and (31) in Eq. (34) yields

$$\frac{\mathrm{d}}{\mathrm{d}t}(\delta\boldsymbol{q}_{\mathrm{B/I}}) \approx \tfrac{1}{2}(\hat{\boldsymbol{\omega}}^{\mathrm{B}}_{\mathrm{B/I}})^{*}\hat{\boldsymbol{q}}^{*}_{\mathrm{B/I}}\boldsymbol{q}_{\mathrm{B/I}} + \tfrac{1}{2}\hat{\boldsymbol{q}}^{*}_{\mathrm{B/I}}\boldsymbol{q}_{\mathrm{B/I}}\boldsymbol{\omega}^{\mathrm{B}}_{\mathrm{B/I}} = -\tfrac{1}{2}\hat{\boldsymbol{\omega}}^{\mathrm{B}}_{\mathrm{B/I}}\delta\boldsymbol{q}_{\mathrm{B/I}} + \tfrac{1}{2}\delta\boldsymbol{q}_{\mathrm{B/I}}\boldsymbol{\omega}^{\mathrm{B}}_{\mathrm{B/I}}. \tag{35}$$

Combining Eqs. (32) and (25) yields

$$\boldsymbol{\omega}^{\mathrm{B}}_{\mathrm{B/I}} = \hat{\boldsymbol{\omega}}^{\mathrm{B}}_{\mathrm{B/I}} + \hat{\boldsymbol{b}}_{\boldsymbol{\omega}} - \boldsymbol{b}_{\boldsymbol{\omega}} - \boldsymbol{\eta}_{\boldsymbol{\omega}}. \tag{36}$$

Finally, inserting Eq. (36) in Eq. (35) results in

$$\frac{\mathrm{d}}{\mathrm{d}t}(\delta\boldsymbol{q}_{\mathrm{B/I}}) \approx -\tfrac{1}{2}\hat{\boldsymbol{\omega}}^{\mathrm{B}}_{\mathrm{B/I}}\delta\boldsymbol{q}_{\mathrm{B/I}} + \tfrac{1}{2}\delta\boldsymbol{q}_{\mathrm{B/I}}\hat{\boldsymbol{\omega}}^{\mathrm{B}}_{\mathrm{B/I}} + \tfrac{1}{2}\delta\boldsymbol{q}_{\mathrm{B/I}}\hat{\boldsymbol{b}}_{\boldsymbol{\omega}} - \tfrac{1}{2}\delta\boldsymbol{q}_{\mathrm{B/I}}\boldsymbol{b}_{\boldsymbol{\omega}} - \tfrac{1}{2}\delta\boldsymbol{q}_{\mathrm{B/I}}\boldsymbol{\eta}_{\boldsymbol{\omega}}. \tag{37}$$

At this point, as in the derivation of the Q-MEKF, reduced state and process noise vectors are selected, namely

$$x_{12} = \begin{bmatrix} \overline{\delta\boldsymbol{q}_{\mathrm{B/I}}} \\ \overline{\boldsymbol{b}}_{\boldsymbol{\omega}} \end{bmatrix} \in \mathbb{R}^{12} \quad \text{and} \quad w_{12} = \begin{bmatrix} \overline{\boldsymbol{\eta}}_{\boldsymbol{\omega}} \\ \overline{\boldsymbol{\eta}}_{\boldsymbol{b}_{\boldsymbol{\omega}}} \end{bmatrix} \in \mathbb{R}^{12}, \tag{38}$$

where $\overline{\delta\boldsymbol{q}_{\mathrm{B/I}}}$ and $\overline{\boldsymbol{b}}_{\boldsymbol{\omega}}$ are the vector parts of $\delta\boldsymbol{q}_{\mathrm{B/I}}$ and $\boldsymbol{b}_{\boldsymbol{\omega}}$, respectively. The state equations

of the DQ-MEKF are then given by the vector parts of Eq. (37) and Eq. (27), yielding

$$f_{12}(x_{12}(t),t) = \begin{bmatrix} \overline{-\frac{1}{2}\hat{\boldsymbol{\omega}}^{\mathrm{B}}_{\mathrm{B/I}}\delta\boldsymbol{q}_{\mathrm{B/I}} + \frac{1}{2}\delta\boldsymbol{q}_{\mathrm{B/I}}\hat{\boldsymbol{\omega}}^{\mathrm{B}}_{\mathrm{B/I}} + \frac{1}{2}\delta\boldsymbol{q}_{\mathrm{B/I}}\hat{\boldsymbol{b}}_{\boldsymbol{\omega}} - \frac{1}{2}\delta\boldsymbol{q}_{\mathrm{B/I}}\boldsymbol{b}_{\boldsymbol{\omega}}} \\ 0_{6\times 1} \end{bmatrix}, \tag{39}$$

$$g_{12\times 12}(x_{12}(t),t) = \begin{bmatrix} -\frac{1}{2}[\widetilde{\delta\boldsymbol{q}_{\mathrm{B/I}}}] & 0_{6\times 6} \\ 0_{6\times 6} & I_{6\times 6} \end{bmatrix}. \tag{40}$$

By replacing the scalar parts $\delta q_{\mathrm{B/I},r,0}$ and $\delta q_{\mathrm{B/I},d,0}$ through Eq. (23) in Eqs. (39) and (40) and using Eq. (5), $F_{12\times 12}(t)$ and $G_{12\times 12}(t)$ can be determined to be

$$F_{12\times 12}(t) = \begin{bmatrix} -\overline{\hat{\boldsymbol{\omega}}^{\mathrm{B}}_{\mathrm{B/I}}}^{\times} & -\frac{1}{2}I_{6\times 6} \\ 0_{6\times 6} & 0_{6\times 6} \end{bmatrix} \quad \text{and} \quad G_{12\times 12}(t) = \begin{bmatrix} -\frac{1}{2}I_{6\times 6} & 0_{6\times 6} \\ 0_{6\times 6} & I_{6\times 6} \end{bmatrix}. \tag{41}$$

III.C.1. Time Update

For the time update of the DQ-MEKF, the $\hat{\boldsymbol{q}}_{\mathrm{B/I}}$, $\hat{\boldsymbol{\omega}}^{\mathrm{B}}_{\mathrm{B/I}}$, and $\hat{\boldsymbol{b}}_{\boldsymbol{\omega}}$ are propagated using Eqs. (31), (32), and (33), respectively, given $\hat{\boldsymbol{q}}_{\mathrm{B/I}}(t_0)$ and $\hat{\boldsymbol{b}}_{\boldsymbol{\omega}}(t_0)$.

Numerical errors in the propagation of $\hat{\boldsymbol{q}}_{\mathrm{B/I}}$ through Eq. (31) can result in the violation of the algebraic constraints specified by Eq. (22). Hence, after each integration step, these algebraic constraints are enforced by calculating

$$[q_{\mathrm{B/I},r}] = \frac{[q_{\mathrm{B/I},r}]}{\|[q_{\mathrm{B/I},r}]\|} \quad \text{and} \quad [q_{\mathrm{B/I},d}] = \left(I_{4\times 4} - \frac{[q_{\mathrm{B/I},r}][q_{\mathrm{B/I},r}]^{\mathsf{T}}}{\|[q_{\mathrm{B/I},r}]\|^2}\right)[q_{\mathrm{B/I},d}], \tag{42}$$

where the latter equation corresponds to the projection of $[q_{\mathrm{B/I},d}]$ onto the subspace orthogonal to $[q_{\mathrm{B/I},r}]$.

As for the covariance matrix of x_{12}, i.e.,

$$\begin{aligned} P_{12\times 12}(t) &\triangleq E\left\{\Delta x_{12}(t)\Delta x_{12}(t)^{\mathsf{T}}\}\right] \\ &\triangleq E\left\{\left(\begin{bmatrix} \overline{\delta\boldsymbol{q}_{\mathrm{B/I}}}(t) \\ \overline{\boldsymbol{b}}_{\boldsymbol{\omega}}(t) \end{bmatrix} - \begin{bmatrix} 0_{6\times 1} \\ \overline{\hat{\boldsymbol{b}}}_{\boldsymbol{\omega}}(t) \end{bmatrix}\right)\left(\begin{bmatrix} \overline{\delta\boldsymbol{q}_{\mathrm{B/I}}}(t) \\ \overline{\boldsymbol{b}}_{\boldsymbol{\omega}}(t) \end{bmatrix} - \begin{bmatrix} 0_{6\times 1} \\ \overline{\hat{\boldsymbol{b}}}_{\boldsymbol{\omega}}(t) \end{bmatrix}\right)^{\mathsf{T}}\right\}, \end{aligned} \tag{43}$$

it is propagated according to Eq. (4) given $P_{12\times 12}(t_0)$ and where

$$Q_{12\times 12}(t) = \begin{bmatrix} \overline{Q}_{\boldsymbol{\omega}}(t) & 0_{6\times 6} \\ 0_{6\times 6} & \overline{Q}_{\boldsymbol{b}_{\boldsymbol{\omega}}}(t) \end{bmatrix}. \tag{44}$$

III.C.2. Measurement Update

In this section, it is assumed that a measurement of $\boldsymbol{q}_{\mathrm{B/I}}$ is available. If the I-frame is a moving frame, this measurement can come, for example, from a vision-based system. If the I-frame is an inertial frame, this measurement can come, for example, from a combination of a star sensor and a GPS. If the pose measurement is available in terms of a quaternion and a translation vector, then the corresponding dual quaternion can be computed from Eq. (21). Then, the output equation is defined analogously to the output equation used in Refs. [4,12] when a quaternion measurement is available, i.e.,

$$\overline{(\hat{\boldsymbol{q}}^{-}_{\mathrm{B/I}}(t_k))^{*}\boldsymbol{q}_{\mathrm{B/I},m}(t_k)} = \overline{\delta\boldsymbol{q}_{\mathrm{B/I}}(t_k)} + v_6(t_k), \tag{45}$$

where, in accordance with Eq. (6), $z_6(t_k) = \overline{(\hat{\boldsymbol{q}}^{-}_{\mathrm{B/I}}(t_k))^{*}\boldsymbol{q}_{\mathrm{B/I},m}(t_k)}$ and $h_6(x_{12}(t_k)) = \overline{\delta\boldsymbol{q}_{\mathrm{B/I}}(t_k)}$. Hence, using Eq. (11) to calculate the measurement sensitivity matrix, yields

$$H_{6\times 12}(t_k) = \begin{bmatrix} I_{6\times 6} & 0_{6\times 6} \end{bmatrix}. \tag{46}$$

In summary, for the measurement update of the DQ-MEKF, the Kalman gain is calculated from Eq. (10), whereas the optimal Kalman state update is calculated from Eq. (8) as

$$\Delta^{\star}\hat{x}_{12}(t_k) \triangleq \begin{bmatrix} \Delta^{\star}\overline{\delta\hat{\boldsymbol{q}}_{\mathrm{B/I}}}(t_k) \\ \Delta^{\star}\overline{\hat{\boldsymbol{b}}}_{\boldsymbol{\omega}}(t_k) \end{bmatrix} = K_{12\times 6}(t_k)(z_6(t_k) - \hat{z}_6(t_k)) = K_{12\times 6}\overline{(\hat{\boldsymbol{q}}^{-}_{\mathrm{B/I}}(t_k))^{*}\boldsymbol{q}_{\mathrm{B/I},m}(t_k)}. \tag{47}$$

The estimate of the state at time t_k after the measurement is then calculated from

$$\hat{\boldsymbol{q}}^{+}_{\mathrm{B/I}}(t_k) = \hat{\boldsymbol{q}}^{-}_{\mathrm{B/I}}(t_k)\Delta^{\star}\delta\hat{\boldsymbol{q}}_{\mathrm{B/I}}(t_k), \tag{48}$$

$$\overline{\hat{\boldsymbol{b}}}^{+}_{\boldsymbol{\omega}}(t_k) = \overline{\hat{\boldsymbol{b}}}^{-}_{\boldsymbol{\omega}}(t_k) + \Delta^{\star}\overline{\hat{\boldsymbol{b}}}_{\boldsymbol{\omega}}(t_k), \tag{49}$$

where $\Delta^{\star}\delta\hat{\boldsymbol{q}}_{\mathrm{B/I}}$ is defined as the unit dual quaternion

$$\Delta^{\star}\delta\hat{\boldsymbol{q}}_{\mathrm{B/I}} = \left(\sqrt{1-\|\Delta^{\star}\overline{\delta\hat{q}_{\mathrm{B/I},r}}\|^2}, \Delta^{\star}\overline{\delta\hat{q}_{\mathrm{B/I},r}}\right) + \epsilon\left(\frac{-\Delta^{\star}\overline{\delta\hat{q}_{\mathrm{B/I},r}}^{\mathsf{T}}\Delta^{\star}\overline{\delta\hat{q}_{\mathrm{B/I},d}}}{\sqrt{1-\|\Delta^{\star}\overline{\delta\hat{q}_{\mathrm{B/I},r}}\|^2}}, \Delta^{\star}\overline{\delta\hat{q}_{\mathrm{B/I},d}}\right). \tag{50}$$

Note that Eq. (50) assumes that the attitude error between the true attitude and its estimate is smaller than 180 deg. Moreover, note that Eq. (50) does not assume that the scalar part of the real part of $\Delta^{\star}\delta\hat{\boldsymbol{q}}_{\mathrm{B/I}}$ is identically one as in Ref. [1], but instead uses the nonlinear quaternion reset suggested in Ref. [4].

If the initial guess of the state is not close enough to the real state, the norm of $\Delta^\star\overline{\delta\hat{q}_{\mathrm{B/I},r}}$ may become larger than one, which will make the scalar part of the quaternions in Eq. (50) complex. Hence, if the norm of $\Delta^\star\overline{\delta\hat{q}_{\mathrm{B/I},r}}$ is larger than one, Eq. (50) is replaced by

$$\Delta^\star\delta\hat{\boldsymbol{q}}_{\mathrm{B/I}}=\left(\frac{1}{\sqrt{1+\|\Delta^\star\overline{\delta\hat{q}_{\mathrm{B/I},r}}\|^2}},\frac{\Delta^\star\overline{\delta\hat{q}_{\mathrm{B/I},r}}}{\sqrt{1+\|\Delta^\star\overline{\delta\hat{q}_{\mathrm{B/I},r}}\|^2}}\right)+\epsilon\left(\frac{-\Delta^\star\overline{\delta\hat{q}_{\mathrm{B/I},r}}^{\mathsf{T}}\Delta^\star\overline{\delta\hat{q}_{\mathrm{B/I},d}}}{1\Big/\sqrt{1+\|\Delta^\star\overline{\delta\hat{q}_{\mathrm{B/I},r}}\|^2}},\Delta^\star\overline{\delta\hat{q}_{\mathrm{B/I},d}}\right).$$

Note that whereas Eq. (49) is a direct application of Eq. (7), Eq. (48) is not. Since $\Delta^\star\delta\hat{\boldsymbol{q}}_{\mathrm{B/I}}(t_k)$ is a unit dual quaternion, $\hat{\boldsymbol{q}}^+_{\mathrm{B/I}}(t_k)$ is calculated using the dual quaternion multiplication, making the proposed EKF multiplicative. Finally, the covariance matrix of the state immediately after the measurement at t_k is computed from Eq. (13).

Any measurement that is a nonlinear function of the state of the DQ-MEKF, i.e., any measurement that satisfies Eq. (6), can be used in the measurement update. If another measurement is used, only the measurement sensitivity matrix given by Eq. (46) needs to be recalculated. For example, if the measurements are $q_{\mathrm{B/I},m}$ and $r^{\mathrm{I}}_{\mathrm{B/I},m}$, then the output equation is defined as

$$\begin{bmatrix}\overline{(\hat{q}^-_{\mathrm{B/I}}(t_k))^*q_{\mathrm{B/I},m}(t_k)}\\ \overline{r^{\mathrm{I}}_{\mathrm{B/I},m}(t_k)}\end{bmatrix}=\begin{bmatrix}\overline{\delta q_{\mathrm{B/I},r}(t_k)}\\ \overline{2\left(\hat{\boldsymbol{q}}_{\mathrm{B/I}}\delta\boldsymbol{q}_{\mathrm{B/I}}\right)_d\delta q^*_{\mathrm{B/I}}\hat{q}_{\mathrm{B/I}}}\end{bmatrix}+v_6(t_k),\tag{51}$$

since $r^{\mathrm{I}}_{\mathrm{B/I}}=2q_{\mathrm{B/I},d}q^*_{\mathrm{B/I}}=2\left(\hat{\boldsymbol{q}}_{\mathrm{B/I}}\delta\boldsymbol{q}_{\mathrm{B/I}}\right)_d\delta q^*_{\mathrm{B/I}}\hat{q}_{\mathrm{B/I}}$. By replacing $\delta q_{\mathrm{B/I},r,0}$ and $\delta q_{\mathrm{B/I},d,0}$ through Eq. (23) in Eq. (51), the new sensitivity matrix can be determined to be

$$H_{6\times12}(t_k)=\begin{bmatrix}I_{3\times3} & 0_{3\times3} & 0_{3\times3} & 0_{3\times3}\\ 0_{3\times3} & 2R\left((\hat{q}^-_{\mathrm{B/I}})^*\right) & 0_{3\times3} & 0_{3\times3}.\end{bmatrix}.\tag{52}$$

III.D. Special Case: No Angular or Linear Velocity Measurements

A special case of particular interest is when pose measurements are available, but angular or linear velocity measurements are not available. Although angular and linear velocity measurements are not available, angular and linear velocity estimates might be required for pose stabilization or tracking.[8] In this section, it is shown how this case can be handled by modifying the inputs and the parameters of the DQ-MEKF algorithm, without any modification to the structure and basic equations of the DQ-MEKF algorithm. This version of the DQ-MEKF is specially suited for satellite proximity operations where the relative pose is measured using vision-based systems, which typically do not provide direct relative velocity measurements.[24] In this scenario, the I-frame is the moving frame of the target satellite.

If angular and linear velocity measurements are not available, but estimates are required, $\boldsymbol{\omega}^{\mathrm{B}}_{\mathrm{B/I},m}$ and $\boldsymbol{\eta}_{\boldsymbol{\omega}}$ are set to zero in Eq. (25). This results in

$$\boldsymbol{b}_{\boldsymbol{\omega}} = -\boldsymbol{\omega}^{\mathrm{B}}_{\mathrm{B/I}} \tag{53}$$

and $\overline{Q}_{\boldsymbol{\omega}} = 0_{6\times 6}$. The dual velocity estimate is still given by Eq. (32), which now has the form $\hat{\boldsymbol{\omega}}^{\mathrm{B}}_{\mathrm{B/I}} = -\hat{\boldsymbol{b}}_{\boldsymbol{\omega}}$. The time derivative of $\boldsymbol{b}_{\boldsymbol{\omega}}$ is still calculated as in Eq. (27). However, since $\boldsymbol{b}_{\boldsymbol{\omega}}$ is now expected to be time-varying and not constant, the effect of the noise $\boldsymbol{\eta}_{\boldsymbol{b}_{\boldsymbol{\omega}}}$ might have to be increased by increasing $\overline{Q}_{\boldsymbol{b}_{\boldsymbol{\omega}}}$.

In summary, this special case can be handled by just setting $\boldsymbol{\omega}^{\mathrm{B}}_{\mathrm{B/I},m}$ and $\overline{Q}_{\boldsymbol{\omega}}$ to zero and, if necessary, by increasing $\overline{Q}_{\boldsymbol{b}_{\boldsymbol{\omega}}}$.

III.E. Special Case: Linear Acceleration Measurements

Unlike the previous case, the structure of the DQ-MEKF algorithm described in Section III.C needs to be modified for the case of a satellite having no means of directly measuring linear velocity, but with the ability to measure linear acceleration using an accelerometer or an Inertial Measurement Unit (IMU). Since an accelerometer measures accelerations with respect to the inertial frame, in this section, the I-frame should be interpreted as an inertial frame. The main modifications compared to the algorithm described in Section III.C are the addition of the bias of the accelerometer to the state of the DQ-MEKF and a new expression for the time derivative of b_v, which in this case is not calculated from Eq. (27). Since angular (but not linear) velocity measurements and linear (but not angular) acceleration measurements are assumed to be available, the duality between the linear and angular motion is broken in this case. Hence, the equations of the DQ-MEKF for this particular case cannot be written compactly in terms of dual quaternions as in Sections III.C and III.D.

First, similarly to the angular and linear velocity measurement model, the linear acceleration measurement model is defined as[11]

$$n^{\mathrm{B}}_{\mathrm{A/I},m} = n^{\mathrm{B}}_{\mathrm{A/I}} + b_n + \eta_n, \tag{54}$$

where $n^{\mathrm{B}}_{\mathrm{A/I}} = (0, \overline{n}^{\mathrm{B}}_{\mathrm{A/I}})$, $\overline{n}^{\mathrm{B}}_{\mathrm{A/I}}$ is the non-dimensional specific force at the location of the accelerometer with respect to the inertial frame expressed in the body frame, $n^{\mathrm{B}}_{\mathrm{A/I},m} = (0, \overline{n}^{\mathrm{B}}_{\mathrm{A/I},m})$, $\overline{n}^{\mathrm{B}}_{\mathrm{A/I},m}$ is a measurement of $\overline{n}^{\mathrm{B}}_{\mathrm{A/I}}$ produced by the accelerometer/IMU, $b_n = (0, \overline{b}_n)$, $\overline{b}_n$ is the bias of the specific force measurement, $\eta_n = (0, \overline{\eta}_n)$, and $\overline{\eta}_n$ is the noise of the specific force measurement assumed to be a Gaussian white-noise process with $E\left\{\overline{\eta}_n(t)\overline{\eta}_n^{\mathrm{T}}(\tau)\right\} = \overline{Q}_n(t)\delta(t-\tau)$, where $\overline{Q}_n(t) \in \mathbb{R}^{3\times 3}$ is a symmetric positive semidefinite matrix. The bias is not constant, but assumed to be driven by another zero-mean Gaussian white noise process

through

$$\dot{b}_n = \eta_{b_n}, \tag{55}$$

where $\eta_{b_n} = (0, \overline{\eta}_{b_n})$, $E\left\{\overline{\eta}_{b_n}\right\} = 0_{3\times 1}$, $E\left\{\overline{\eta}_{b_n}(t)\overline{\eta}_{b_n}^{\mathsf{T}}(\tau)\right\} = \overline{Q}_{b_n}(t)\delta(t-\tau)$, and $\overline{Q}_{b_n}(t) \in \mathbb{R}^{3\times 3}$ is a symmetric positive semidefinite matrix. From Eq. (54), the expected value of $n^{\mathrm{B}}_{\mathrm{A/I}}$ is given by

$$\hat{n}^{\mathrm{B}}_{\mathrm{A/I}} = n^{\mathrm{B}}_{\mathrm{A/I},m} - \hat{b}_n, \tag{56}$$

where $\hat{b}_n \triangleq E\{b_n\}$. Likewise,

$$\frac{\mathrm{d}}{\mathrm{d}t}\left(\hat{b}_n\right) = E\{\eta_{b_n}\} = 0. \tag{57}$$

Moreover, combining Eqs. (54) and (56) yields

$$n^{\mathrm{B}}_{\mathrm{A/I}} = \hat{n}^{\mathrm{B}}_{\mathrm{A/I}} + \hat{b}_n - b_n - \eta_n. \tag{58}$$

The state and process noise of the DQ-MEKF are now selected as

$$x_{20} = \begin{bmatrix}[\delta \boldsymbol{q}_{\mathrm{B/I}}]^{\mathsf{T}} & [\boldsymbol{b}_{\boldsymbol{\omega}}]^{\mathsf{T}} & [b_n]^{\mathsf{T}}\end{bmatrix}^{\mathsf{T}} \in \mathbb{R}^{20} \text{ and } w_{20} = \begin{bmatrix}[\boldsymbol{\eta}_{\boldsymbol{\omega}}]^{\mathsf{T}} & [\eta_{b_\omega}]^{\mathsf{T}} & [\eta_n]^{\mathsf{T}} & [\eta_{b_n}]^{\mathsf{T}}\end{bmatrix}^{\mathsf{T}} \in \mathbb{R}^{20}, \tag{59}$$

where the state equation for $\delta \boldsymbol{q}_{\mathrm{B/I}}$ is given by Eq. (37) and the state equation for b_ω, i.e., the real part of $\boldsymbol{b}_{\boldsymbol{\omega}}$, is given as in Eq. (27) by $\dot{b}_\omega = \eta_{b_\omega}$, which implies that

$$\frac{\mathrm{d}}{\mathrm{d}t}\left(\hat{b}_\omega\right) = E\{\eta_{b_\omega}\} = 0. \tag{60}$$

Whereas in Section III.C, the time derivative of b_v was also calculated from Eq. (27), here the time derivative of b_v is calculated as follows. Since there are no linear velocity measurements, $v^{\mathrm{B}}_{\mathrm{B/I},m}$ and η_v are set to zero (as in Section III.D) in Eq. (25), resulting in $b_v = -v^{\mathrm{B}}_{\mathrm{B/I}}$ and $\overline{Q}_v = \overline{Q}_{\omega v} = 0_{3\times 3}$. This, in turn, implies that

$$\hat{v}^{\mathrm{B}}_{\mathrm{B/I}} = -\hat{b}_v. \tag{61}$$

Taking the time derivative of both sides of $b_v = -v^{\mathrm{B}}_{\mathrm{B/I}}$ leads to $\dot{b}_v = -\dot{v}^{\mathrm{B}}_{\mathrm{B/I}}$. Note that $\dot{v}^{\mathrm{B}}_{\mathrm{B/I}}$ is related to $n^{\mathrm{B}}_{\mathrm{A/I}}$ through

$$\dot{v}^{\mathrm{B}}_{\mathrm{B/I}} = -\omega^{\mathrm{B}}_{\mathrm{B/I}} \times v^{\mathrm{B}}_{\mathrm{B/I}} + c n^{\mathrm{B}}_{\mathrm{A/I}} - q^*_{\mathrm{B/I}} g^{\mathrm{I}} q_{\mathrm{B/I}} - \alpha^{\mathrm{B}}_{\mathrm{B/I}} \times r^{\mathrm{B}}_{\mathrm{A/B}} - \omega^{\mathrm{B}}_{\mathrm{B/I}} \times (\omega^{\mathrm{B}}_{\mathrm{B/I}} \times r^{\mathrm{B}}_{\mathrm{A/B}}), \tag{62}$$

where $c \in \mathbb{R}$ is a scaling constant specific to each accelerometer, $g^{\mathrm{I}} = (0, \overline{g}^{\mathrm{I}})$, $\overline{g}^{\mathrm{I}}$ is the local gravity acceleration vector expressed in the inertial frame (assumed to be known), $\alpha^{\mathrm{B}}_{\mathrm{B/I}} = (0, \overline{\alpha}^{\mathrm{B}}_{\mathrm{B/I}})$, $\overline{\alpha}^{\mathrm{B}}_{\mathrm{B/I}}$ is the angular acceleration of the body frame with respect to the inertial frame expressed in the body frame, $r^{\mathrm{B}}_{\mathrm{A/B}} = (0, \overline{r}^{\mathrm{B}}_{\mathrm{A/B}})$, and $\overline{r}^{\mathrm{B}}_{\mathrm{A/B}}$ is the translation vector from

the origin of the body frame to the accelerometer expressed in the body frame (assumed to be known). Hence, $\dot{b}_v = -\dot{v}^{\mathrm{B}}_{\mathrm{B/I}} = -\omega^{\mathrm{B}}_{\mathrm{B/I}} \times b_v - cn^{\mathrm{B}}_{\mathrm{A/I}} + q^*_{\mathrm{B/I}} g^{\mathrm{I}} q_{\mathrm{B/I}} + \alpha^{\mathrm{B}}_{\mathrm{B/I}} \times r^{\mathrm{B}}_{\mathrm{A/B}} + \omega^{\mathrm{B}}_{\mathrm{B/I}} \times (\omega^{\mathrm{B}}_{\mathrm{B/I}} \times r^{\mathrm{B}}_{\mathrm{A/B}})$. Finally, neglecting $\alpha^{\mathrm{B}}_{\mathrm{B/I}}$, which is assumed to be unknown, and using Eq. (58) and the real parts of Eqs. (30) and (36), results in

$$
\begin{aligned}
\dot{b}_v =& -\dot{v}^{\mathrm{B}}_{\mathrm{B/I}} \approx -(\hat{\omega}^{\mathrm{B}}_{\mathrm{B/I}} + \hat{b}_\omega - b_\omega - \eta_\omega) \times b_v - c(\hat{n}^{\mathrm{B}}_{\mathrm{A/I}} + \hat{b}_n - b_n - \eta_n) + \delta q^*_{\mathrm{B/I}} \hat{q}^*_{\mathrm{B/I}} g^{\mathrm{I}} \hat{q}_{\mathrm{B/I}} \delta q_{\mathrm{B/I}} \\
&+ (\hat{\omega}^{\mathrm{B}}_{\mathrm{B/I}} + \hat{b}_\omega - b_\omega - \eta_\omega) \times ((\hat{\omega}^{\mathrm{B}}_{\mathrm{B/I}} + \hat{b}_\omega - b_\omega - \eta_\omega) \times r^{\mathrm{B}}_{\mathrm{A/B}}) \\
=& -(\hat{\omega}^{\mathrm{B}}_{\mathrm{B/I}} + \hat{b}_\omega - b_\omega) \times b_v - c(\hat{n}^{\mathrm{B}}_{\mathrm{A/I}} + \hat{b}_n - b_n) + \delta q^*_{\mathrm{B/I}} \hat{q}^*_{\mathrm{B/I}} g^{\mathrm{I}} \hat{q}_{\mathrm{B/I}} \delta q_{\mathrm{B/I}} \\
&+ (\hat{\omega}^{\mathrm{B}}_{\mathrm{B/I}} + \hat{b}_\omega - b_\omega) \times ((\hat{\omega}^{\mathrm{B}}_{\mathrm{B/I}} + \hat{b}_\omega - b_\omega) \times r^{\mathrm{B}}_{\mathrm{A/B}}) \\
&- b_v \times \eta_\omega + c\eta_n - \eta_\omega \times ((\hat{\omega}^{\mathrm{B}}_{\mathrm{B/I}} + \hat{b}_\omega - b_\omega) \times r^{\mathrm{B}}_{\mathrm{A/B}}) + (\hat{\omega}^{\mathrm{B}}_{\mathrm{B/I}} + \hat{b}_\omega - b_\omega) \times (-\eta_\omega \times r^{\mathrm{B}}_{\mathrm{A/B}}) \\
&+ (-\eta_\omega) \times (-\eta_\omega \times r^{\mathrm{B}}_{\mathrm{A/B}}).
\end{aligned} \tag{63}
$$

The last term of Eq. (63) is quadratic with respect to η_ω and, hence, does not have the same form as Eq. (1). Since the typical EKF formulation does not account for terms quadratic with respect to the process noise, this term is neglected.

Note that by using the typical approximation given by Eq. (2), the time derivative of $\hat{b}_v$ can be calculated from Eq. (63) to be

$$
\dot{\hat{b}}_v \approx -\hat{\omega}^{\mathrm{B}}_{\mathrm{B/I}} \times \hat{b}_v - c\hat{n}^{\mathrm{B}}_{\mathrm{A/I}} + \hat{q}^*_{\mathrm{B/I}} g^{\mathrm{I}} \hat{q}_{\mathrm{B/I}} + \hat{\omega}^{\mathrm{B}}_{\mathrm{B/I}} \times (\hat{\omega}^{\mathrm{B}}_{\mathrm{B/I}} \times r^{\mathrm{B}}_{\mathrm{A/B}}). \tag{64}
$$

At this point, as before, reduced state and process noise vectors are selected, namely

$$
x_{15} = \begin{bmatrix} \overline{\delta \boldsymbol{q}_{\mathrm{B/I}}}^{\mathsf{T}} & \overline{\boldsymbol{b}}^{\mathsf{T}}_{\boldsymbol{\omega}} & \overline{b}^{\mathsf{T}}_n \end{bmatrix}^{\mathsf{T}} \in \mathbb{R}^{15} \text{ and } w_{15} = \begin{bmatrix} \overline{\boldsymbol{\eta}}^{\mathsf{T}}_{\boldsymbol{\omega}} & \overline{\eta}^{\mathsf{T}}_{b_\omega} & \overline{\eta}^{\mathsf{T}}_n & \overline{\eta}^{\mathsf{T}}_{b_n} \end{bmatrix}^{\mathsf{T}} \in \mathbb{R}^{15}. \tag{65}
$$

The state equations of the DQ-MEKF when linear acceleration measurements are available are then given by $f_{15}(x_{15}(t), t)$ and $g_{15\times 15}(x_{15}(t), t)$, defined, respectively, as

$$
\begin{bmatrix}
\overline{-\frac{1}{2}\hat{\boldsymbol{\omega}}^{\mathrm{B}}_{\mathrm{B/I}} \delta \boldsymbol{q}_{\mathrm{B/I}} + \frac{1}{2}\delta \boldsymbol{q}_{\mathrm{B/I}} \hat{\boldsymbol{\omega}}^{\mathrm{B}}_{\mathrm{B/I}} + \frac{1}{2}\delta \boldsymbol{q}_{\mathrm{B/I}} \hat{\boldsymbol{b}}_{\boldsymbol{\omega}} - \frac{1}{2}\delta \boldsymbol{q}_{\mathrm{B/I}} \boldsymbol{b}_{\boldsymbol{\omega}}} \\
0_{3\times 1} \\
\hline
-(\hat{\omega}^{\mathrm{B}}_{\mathrm{B/I}} + \hat{b}_\omega - b_\omega) \times b_v - c(\hat{n}^{\mathrm{B}}_{\mathrm{A/I}} + \hat{b}_n - b_n) + \delta q^*_{\mathrm{B/I}} \hat{q}^*_{\mathrm{B/I}} g^{\mathrm{I}} \hat{q}_{\mathrm{B/I}} \delta q_{\mathrm{B/I}} + (\hat{\omega}^{\mathrm{B}}_{\mathrm{B/I}} + \hat{b}_\omega - b_\omega) \times ((\hat{\omega}^{\mathrm{B}}_{\mathrm{B/I}} + \hat{b}_\omega - b_\omega) \times r^{\mathrm{B}}_{\mathrm{A/B}}) \\
0_{3\times 1}
\end{bmatrix},
$$

$$\begin{bmatrix} -\frac{1}{2}[\widetilde{\delta \boldsymbol{q}_{\mathrm{B/I},r}}] & 0_{3\times3} & 0_{3\times3} & 0_{3\times3} & 0_{3\times3} \\ -\frac{1}{2}[\widetilde{\delta \boldsymbol{q}_{\mathrm{B/I},d}}] & -\frac{1}{2}[\widetilde{\delta \boldsymbol{q}_{\mathrm{B/I},r}}] & 0_{3\times3} & 0_{3\times3} & 0_{3\times3} \\ 0_{3\times3} & 0_{3\times3} & I_{3\times3} & 0_{3\times3} & 0_{3\times3} \\ -\overline{b_v}^{\times} + \overline{(\hat{\omega}^{\mathrm{B}}_{\mathrm{B/I}} + \hat{b}_\omega - b_\omega)\times r^{\mathrm{B}}_{\mathrm{A/B}}}^{\times} + \overline{\hat{\omega}^{\mathrm{B}}_{\mathrm{B/I}} + \hat{b}_\omega - b_\omega}^{\times} \overline{r^{\mathrm{B}}_{\mathrm{A/B}}}^{\times} & 0_{3\times3} & 0_{3\times3} & cI_{3\times3} & 0_{3\times3} \\ 0_{3\times3} & 0_{3\times3} & 0_{3\times3} & 0_{3\times3} & I_{3\times3} \end{bmatrix}.$$

By replacing $\delta q_{\mathrm{B/I},r,0}$ and $\delta q_{\mathrm{B/I},d,0}$ through Eq. (23) in $f_{15}(x_{15}(t),t)$ and $g_{15\times15}(x_{15}(t),t)$ and using Eq. (5), $F_{15\times15}(t)$ and $G_{15\times15}(t)$ can be determined to be

$$F_{15\times15}(t) = \begin{bmatrix} -\overline{\hat{\omega}^{\mathrm{B}}_{\mathrm{B/I}}}^{\times} & 0_{3\times3} & -\frac{1}{2}I_{3\times3} & 0_{3\times3} & 0_{3\times3} \\ -\overline{\hat{v}^{\mathrm{B}}_{\mathrm{B/I}}}^{\times} & -\overline{\hat{\omega}^{\mathrm{B}}_{\mathrm{B/I}}}^{\times} & 0_{3\times3} & -\frac{1}{2}I_{3\times3} & 0_{3\times3} \\ 0_{3\times3} & 0_{3\times3} & 0_{3\times3} & 0_{3\times3} & 0_{3\times3} \\ 2\overline{\hat{q}^{*}_{\mathrm{B/I}} g^{\mathrm{I}} \hat{q}_{\mathrm{B/I}}}^{\times} & 0_{3\times3} & -\overline{\hat{b}_v}^{\times} + \overline{\hat{\omega}^{\mathrm{B}}_{\mathrm{B/I}} \times r^{\mathrm{B}}_{\mathrm{A/B}}}^{\times} + \overline{\hat{\omega}^{\mathrm{B}}_{\mathrm{B/I}}}^{\times} \overline{r^{\mathrm{B}}_{\mathrm{A/B}}}^{\times} & -\overline{\hat{\omega}^{\mathrm{B}}_{\mathrm{B/I}}}^{\times} & cI_{3\times3} \\ 0_{3\times3} & 0_{3\times3} & 0_{3\times3} & 0_{3\times3} & 0_{3\times3} \end{bmatrix} \tag{66}$$

and

$$G_{15\times15}(t) = \begin{bmatrix} -\frac{1}{2}I_{3\times3} & 0_{3\times3} & 0_{3\times3} & 0_{3\times3} & 0_{3\times3} \\ 0_{3\times3} & -\frac{1}{2}I_{3\times3} & 0_{3\times3} & 0_{3\times3} & 0_{3\times3} \\ 0_{3\times3} & 0_{3\times3} & I_{3\times3} & 0_{3\times3} & 0_{3\times3} \\ -\overline{\hat{b}_v}^{\times} + \overline{\hat{\omega}^{\mathrm{B}}_{\mathrm{B/I}} \times r^{\mathrm{B}}_{\mathrm{A/B}}}^{\times} + \overline{\hat{\omega}^{\mathrm{B}}_{\mathrm{B/I}}}^{\times} \overline{r^{\mathrm{B}}_{\mathrm{A/B}}}^{\times} & 0_{3\times3} & 0_{3\times3} & cI_{3\times3} & 0_{3\times3} \\ 0_{3\times3} & 0_{3\times3} & 0_{3\times3} & 0_{3\times3} & I_{3\times3} \end{bmatrix}. \tag{67}$$

III.E.1. Time Update

When acceleration measurements are available, for the time update of the DQ-MEKF, $\hat{\boldsymbol{q}}_{\mathrm{B/I}}$, $\hat{b}_\omega$, $\hat{b}_v$, $\hat{b}_n$, $\hat{v}^{\mathrm{B}}_{\mathrm{B/I}}$, $\hat{\omega}^{\mathrm{B}}_{\mathrm{B/I}}$ are propagated using Eqs. (31), (60), (64), (57), (61), and the real part of Eq. (32), i.e., $\hat{\omega}^{\mathrm{B}}_{\mathrm{B/I}} = \omega^{\mathrm{B}}_{\mathrm{B/I},m} - \hat{b}_\omega$, respectively, given $\hat{\boldsymbol{q}}_{\mathrm{B/I}}(t_0)$, $\hat{\boldsymbol{b}}_{\boldsymbol{\omega}}(t_0)$, and $\hat{b}_n(t_0)$.

Numerical errors in the propagation of $\hat{\boldsymbol{q}}_{\mathrm{B/I}}$ through Eq. (31) can result in the violation of the algebraic constraints specified by Eq. (22). Hence, after each integration step, these algebraic constraints are enforced by using Eq. (42).

As for the covariance matrix of x_{15},

$$P_{15\times15}(t) = E\left\{ \left(\begin{bmatrix} \overline{\delta \boldsymbol{q}_{\mathrm{B/I}}}(t) \\ \overline{\boldsymbol{b}}_{\boldsymbol{\omega}}(t) \\ \overline{b}_n(t) \end{bmatrix} - \begin{bmatrix} 0_{6\times1} \\ \overline{\hat{\boldsymbol{b}}}_{\boldsymbol{\omega}}(t) \\ \overline{\hat{b}}_n(t) \end{bmatrix} \right) \left(\begin{bmatrix} \overline{\delta \boldsymbol{q}_{\mathrm{B/I}}}(t) \\ \overline{\boldsymbol{b}}_{\boldsymbol{\omega}}(t) \\ \overline{b}_n(t) \end{bmatrix} - \begin{bmatrix} 0_{6\times1} \\ \overline{\hat{\boldsymbol{b}}}_{\boldsymbol{\omega}}(t) \\ \overline{\hat{b}}_n(t) \end{bmatrix} \right)^{\mathsf{T}} \right\}, \tag{68}$$

it is propagated according to Eq. (4) given $P_{15\times15}(t_0)$, and where

$$Q_{15\times15}(t) = \begin{bmatrix} \overline{Q}_{\omega}(t) & 0_{3\times3} & 0_{3\times3} & 0_{3\times3} & 0_{3\times3} \\ 0_{3\times3} & 0_{3\times3} & 0_{3\times3} & 0_{3\times3} & 0_{3\times3} \\ 0_{3\times3} & 0_{3\times3} & \overline{Q}_{b_\omega}(t) & 0_{3\times3} & 0_{3\times3} \\ 0_{3\times3} & 0_{3\times3} & 0_{3\times3} & \overline{Q}_{n}(t) & 0_{3\times3} \\ 0_{3\times3} & 0_{3\times3} & 0_{3\times3} & 0_{3\times3} & \overline{Q}_{b_n}(t) \end{bmatrix}. \tag{69}$$

III.E.2. Measurement Update

When acceleration measurements are available, the measurement update is performed as in Section III.C with the measurement sensitivity matrix now given by

$$H_{6\times15}(t_k) = \begin{bmatrix} I_{6\times6} & 0_{6\times6} & 0_{6\times3} \end{bmatrix}. \tag{70}$$

The optimal Kalman state update is now calculated based on Eq. (8) from

$$\Delta^\star\hat{x}_{15}(t_k) \triangleq \begin{bmatrix} \Delta^\star\overline{\delta\hat{\boldsymbol{q}}_{\mathrm{B/I}}}(t_k) \\ \Delta^\star\overline{\hat{\boldsymbol{b}}}_{\boldsymbol{\omega}}(t_k) \\ \Delta^\star\overline{\hat{b}}_{n}(t_k) \end{bmatrix} = K_{15\times6}(t_k)(z_6(t_k) - \hat{z}_6(t_k)) = K_{15\times6}\overline{(\hat{\boldsymbol{q}}^-_{\mathrm{B/I}}(t_k))^*\boldsymbol{q}_{\mathrm{B/I},m}(t_k)}. \tag{71}$$

Finally, the estimate of the state at time t_k after the measurement is calculated from Eqs. (48), (49), and $\overline{\hat{b}}^+_n(t_k) = \overline{\hat{b}}^-_n(t_k) + \Delta^\star\overline{\hat{b}}_n(t_k)$.

IV. Experimental Results

In this section, the two special cases of the DQ-MEKF are validated experimentally on the Autonomous Spacecraft Testing of Robotic Operations in Space (ASTROS) facility at the School of Aerospace Engineering of the Georgia Institute of Technology. This experimental facility includes a 5-DOF platform supported on hemispherical and linear air-bearings moving over a flat epoxy floor in order to simulate as best as possible the frictionless environment of space. The experimental facility also includes a VICON motion capture system mounted on an aluminum grid above the experimental area. The VICON system measures the attitude and position of the platform with respect to a reference frame fixed to the room. These measurements are then transmitted wirelessly to the platform. A picture of the platform is shown in Fig. 3. More information about the ASTROS facility and its 5-DOF platform can be found in Refs. [25, 26]. The most relevant characteristics of the sensors used in the experiments are summarized in Table 1, where SD stands for Standard Deviation. The scaling

constant of the IMU is $c = 9.8$ m/s^2 and it is located at $r^{\mathrm{B}}_{\mathrm{A/B}} = [0.113, -0.016, -0.089]^{\intercal}$ (m).

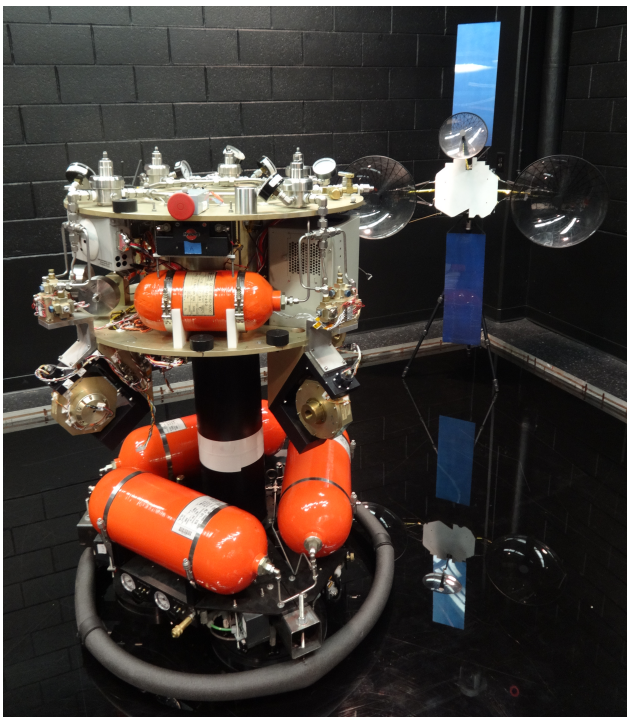

Figure 3. The 5-DOF experimental platform of the ASTROS facility.

Table 1. Characteristics of the sensors.

Meas.	Sensor	Noise SD	Bias	Refresh Rate
$\bar{\omega}^{\mathrm{B}}_{\mathrm{B/I},m}$	Humphrey RG02-3227-1 rate-gyro	0.027 deg/s	<2 deg/s	100 Hz
$\bar{n}^{\mathrm{B}}_{\mathrm{A/I},m}$	Crossbow AHRS400CC-100 IMU	1.5 mg	<8.5 mg	100 Hz
$q_{\mathrm{B/I},m}$	8 VICON Bonita B10 cameras	$< 7 \times 10^{-5}$	-	Variable ($\leq$ 250 Hz)
$\bar{r}^{\mathrm{I}}_{\mathrm{B/I},m}$	8 VICON Bonita B10 cameras	$<$ 1 mm	-	Variable ($\leq$ 250 Hz)

The ground truth for attitude and position was obtained from VICON measurements at 100 Hz. The ground truth for linear velocity was obtained by passing these position measurements through a Linear Time-Invariant (LTI) system with transfer matrix $H(s) = 3s/(s+3)I_{3\times 3}$. The position of the pole was chosen by trial-and-error to minimize noise and lag. Finally, the ground truth for the angular velocity was obtained by passing the quaternion measurements through an LTI system with transfer matrix $H(s) = 3s/(s+3)I_{4\times 4}$ and by using the relation $\omega^{\mathrm{B}}_{\mathrm{B/I}} = 2q^{*}_{\mathrm{B/I}}\dot{q}_{\mathrm{B/I}}$. Note that whereas the LTI filters can reduce the noise at

the cost of lag, the ground truth for linear and angular velocity will still have some noise.

IV.A. DQ-MEKF With No Angular and Linear Velocity Measurements

For this experiment, the DQ-MEKF was fed attitude and position measurements from the VICON system at 10 Hz modeled through the output equation given by Eq. (51). The initial estimate of the state is given in Table 2. The same table also shows an a posteriori guess of the initial state based on the measurements. The DQ-MEKF was initialized with the covariance matrices given in Table 3.

Table 2. Case 1: Initial estimate and a posteriori guess of the state.

Variable	Initial Estimate	A Posteriori Guess
$q_{\mathrm{B/I}}(0)$	$[0.7071, 0, 0, 0.7071]^\intercal$ (-)	$[0.7987, -0.0221, -0.0195, 0.6009]^\intercal$ (-)
$\bar{r}^{\mathrm{I}}_{\mathrm{B/I}}(0)$	$[-0.5, 2, -1]^\intercal$ (m)	$[-0.5256, 2.0425, -0.9887]^\intercal$ (m)
$\bar{b}_\omega(0)$	$[0, 0, 0]^\intercal$ (deg/s)	$[0, 0, 0]^\intercal$ (deg/s)
$\bar{b}_v(0)$	$[0, 0, 0]^\intercal$ (m/s)	$[0, 0, 0]^\intercal$ (m/s)

Table 3. Case 1: Covariance matrices.

$P_{12\times12}(0)$	$\mathrm{diag}([1\times10^{-9}, 1\times10^{-9}, 1\times10^{-9}, 1\times10^{-9}, 1\times10^{-9}, 1\times10^{-9}, 1\times10^{-9}, 1\times10^{-9}, 1\times10^{-9}, 1\times10^{-9}, 1\times10^{-9}, 1\times10^{-9}])$
$Q_{12\times12}$	$\mathrm{diag}([0, 0, 0, 0, 0, 0, 1\times10^{-3}, 1\times10^{-3}, 1\times10^{-3}, 1\times10^{-1}, 1\times10^{-1}, 1\times10^{-1}])$
$R_{6\times6}$	$\mathrm{diag}([1.4\times10^{-6}, 1.4\times10^{-6}, 1.4\times10^{-6}, 2.25\times10^{-6}, 2.25\times10^{-6}, 2.25\times10^{-6}])$

The pose estimated by the DQ-MEKF is compared with the ground truth in Fig. 4. The two appear almost identical. This is to be expected due to the relatively high update rate of pose measurements in this case. Note that the motion only starts around 20 sec after the beginning of the experiment.

The pose estimation error obtained with the DQ-MEKF is plotted in Fig. 5. Note that the pose error increases at around 20 sec, when the motion starts. The same figure also shows the pose estimation error obtained with two alternative EKF formulations.

This first alternative EKF formulation, hereby referred to as the QV-AEKF, is an additive EKF, where the state contains the vector part of the unit error quaternion (like in the Q-MEKF) and the position vector of the body with respect to the inertial frame expressed in the body frame. The QV-AEKF is derived in detail in Appendix A. The biggest differences between the DQ-MEKF and the QV-AEKF are that in the former the position is represented by the dual part of the dual quaternion and the position measurement update is performed using the dual quaternion multiplication, whereas in the latter the position is represented

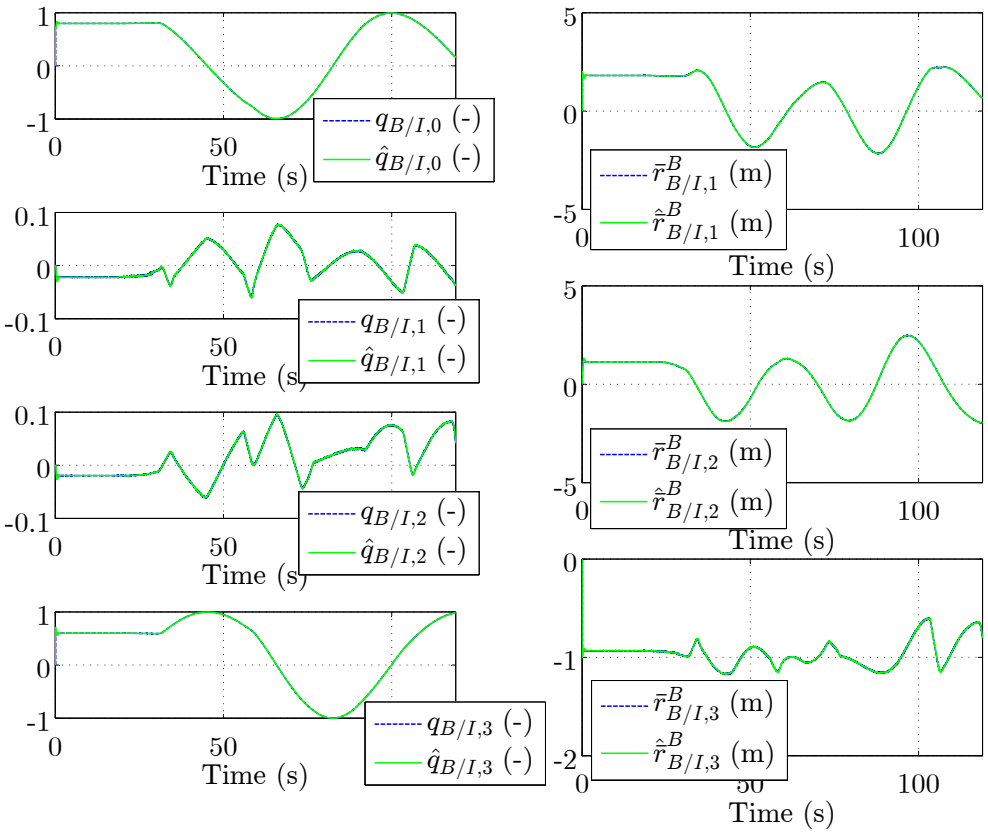

Figure 4. Case 1: estimated and true pose (pose measurements at 10 Hz).

by the body coordinates of the position vector and the position measurement update is performed by adding the optimal correction to the current best estimate.

The second alternative EKF formulation, hereby referred to as the SQV-AEKF, is essentially the QV-AEKF split into two additive EKFs, one for the attitude and another one for the position. The SQV-AEKF is derived in detail in Appendix B.

For the comparison between the DQ-MEKF, the QV-AEKF, and the SQV-AEKF to be fair, the three filters were fed the same measurements, were initialized with the same initial estimate of the state (given in Table 2), and were tuned with the same covariance matrices (given in Table 3).

The linear and angular velocity estimation errors obtained with the three filters are shown in Fig. 6.

The Root-Mean-Square (RMS) attitude, position, angular velocity, and linear velocity estimation errors after 20 sec obtained with the three filters are given in Table 4. Note that the RMS attitude and angular velocity estimation errors obtained with the three filters are the same. This is not surprising since the DQ-MEKF, the QV-AEKF, and the SQV-AEKF represent and update the attitude in the same way and the attitude is independent from the position. However, whereas the RMS position and linear velocity estimation errors obtained

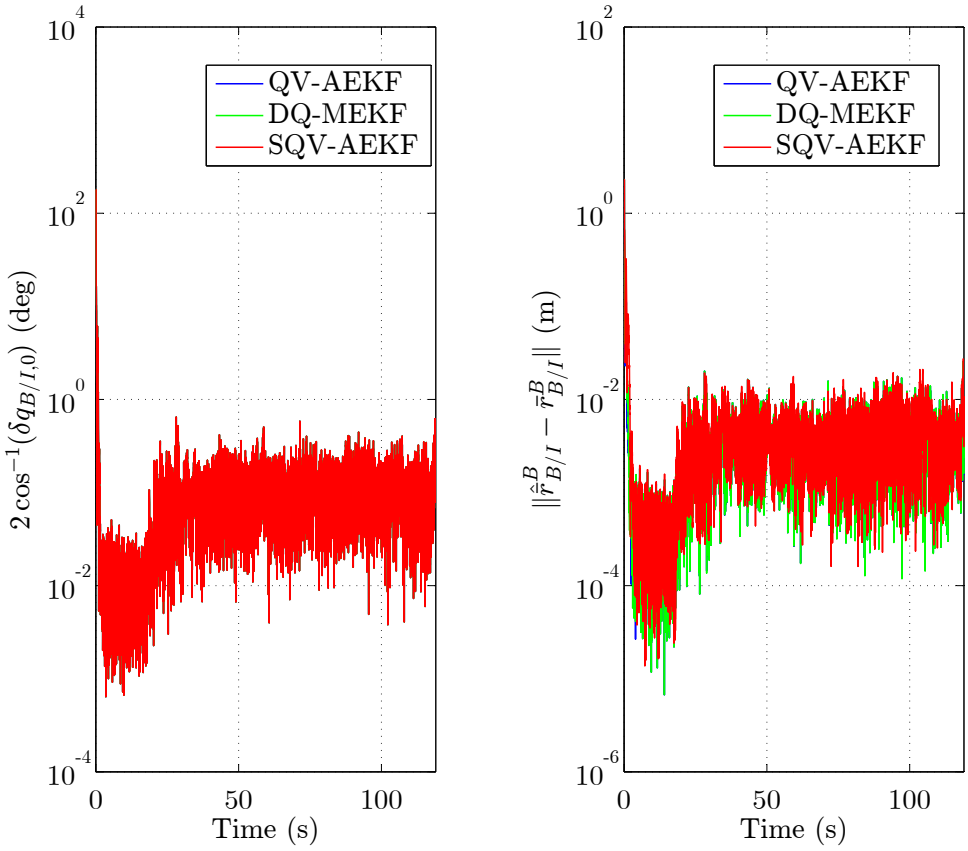

Figure 5. Case 1: pose estimation error (pose measurements at 10 Hz).

with the DQ-MEKF and the QV-AEKF are the same, the RMS position and linear velocity estimation errors obtained with the SQV-AEKF are higher. This is understandable since the DQ-MEKF and the QV-AEKF take into consideration the fact that the position vector of the body with respect to the inertial frame expressed in the body frame depends on the attitude of the body, whereas the SQV-AEKF does not. Another way to see this is to realize that some of the elements of Eqs. (75) and (79) do not appear in Eqs. (83), (90), (87), and (94).

Table 4. Case 1: RMS estimation errors after 20 sec obtained with the three filters (pose measurements at 10 Hz).

RMS Estimation Error	DQ-MEKF	QV-AEKF	SQV-AEKF
Attitude (deg)	0.13	0.13	0.13
Position (mm)	4.5	4.5	5.1
Angular Velocity (deg/s)	0.44	0.44	0.44
Linear Velocity (mm/s)	4.4	4.4	12.6

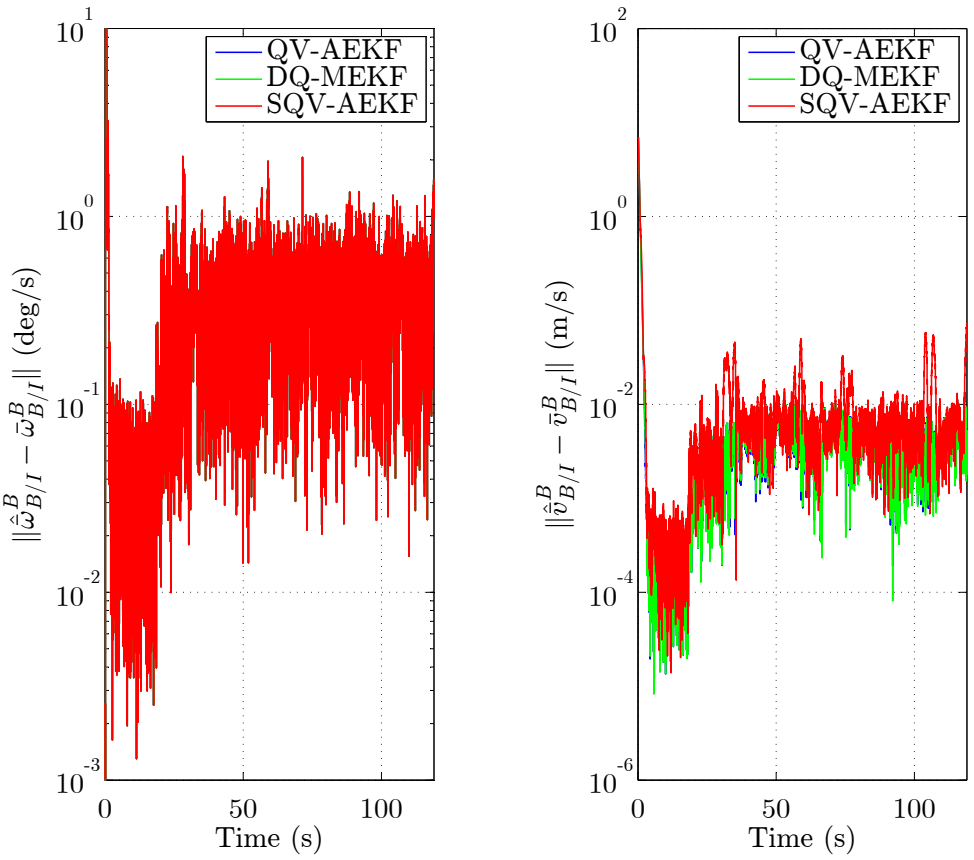

Figure 6. Case 1: angular and linear velocity estimation errors (pose measurements at 10 Hz).

To compare the filters in a more demanding scenario, the same experimental data were fed into the DQ-MEKF, the QV-AEKF, and the SQV-AEKF, but now with an update rate of 0.5 Hz. All other parameters were kept the same. The pose estimated by the DQ-MEKF is compared with the ground truth in Fig. 7. As expected, the pose estimation error in this case is visibly higher than in Fig. 4.

The attitude, position, angular velocity, and linear velocity estimation errors obtained with the DQ-MEKF, the QV-AEKF, and the SQV-AEKF are compared in Fig. 8, Fig. 9, and Table 5. Like in Table 4, the RMS attitude and angular velocity estimation errors obtained with the three filters are the same, and the SQV-AEKF exhibits the highest RMS position and linear velocity estimation errors. However, unlike in Table 4, the RMS position and linear velocity estimation errors obtained with the DQ-MEKF are smaller than the ones obtained with the QV-AEKF. In other words, as the update rate of the pose measurements decreases, the DQ-MEKF starts producing better position and linear velocity estimates than the QV-AEKF. This can be justified in part by Fig. 1. Since the relation between $r^{\mathrm{B}}_{\mathrm{B/I}}$ and $r^{\mathrm{I}}_{\mathrm{B/I}}$ is quadratic in $q_{\mathrm{B/I}}$, whereas the relation between $q_{\mathrm{B/I},d}$ and $r^{\mathrm{I}}_{\mathrm{B/I}}$ is linear in $q_{\mathrm{B/I}}$, the linearization error committed when linearizing the output equations of the QV-AEKF and

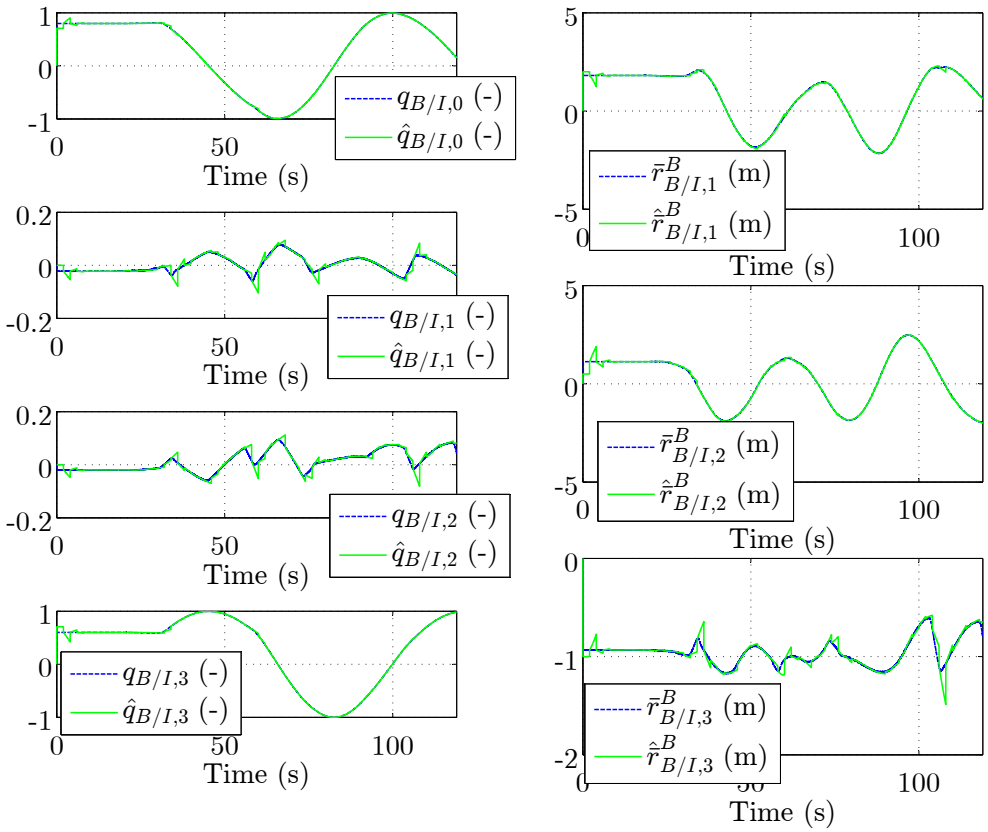

Figure 7. Case 1: estimated and true pose (pose measurements at 0.5 Hz).

of the DQ-MEKF (i.e., Eq. (78) and Eq. (51), respectively) with respect to $\delta q_{\mathrm{B/I}}$ is smaller in the DQ-MEKF case.

Table 5. Case 1: RMS estimation errors after 20 sec obtained with the three filters (pose measurements at 0.5 Hz).

RMS Estimation Error	DQ-MEKF	QV-AEKF	SQV-AEKF
Attitude (deg)	2.22	2.22	2.22
Position (mm)	70.8	69.5	122.8
Angular Velocity (deg/s)	1.91	1.91	1.91
Linear Velocity (mm/s)	22.7	22.2	80.7

IV.B. DQ-MEKF With Linear Acceleration Measurements

For this experiment, the DQ-MEKF was fed attitude and position measurements from the VICON system at 1 Hz, linear acceleration measurements from the IMU at 100 Hz, and angular velocity measurements from the rate-gyro at 100 Hz. The initial estimate of the

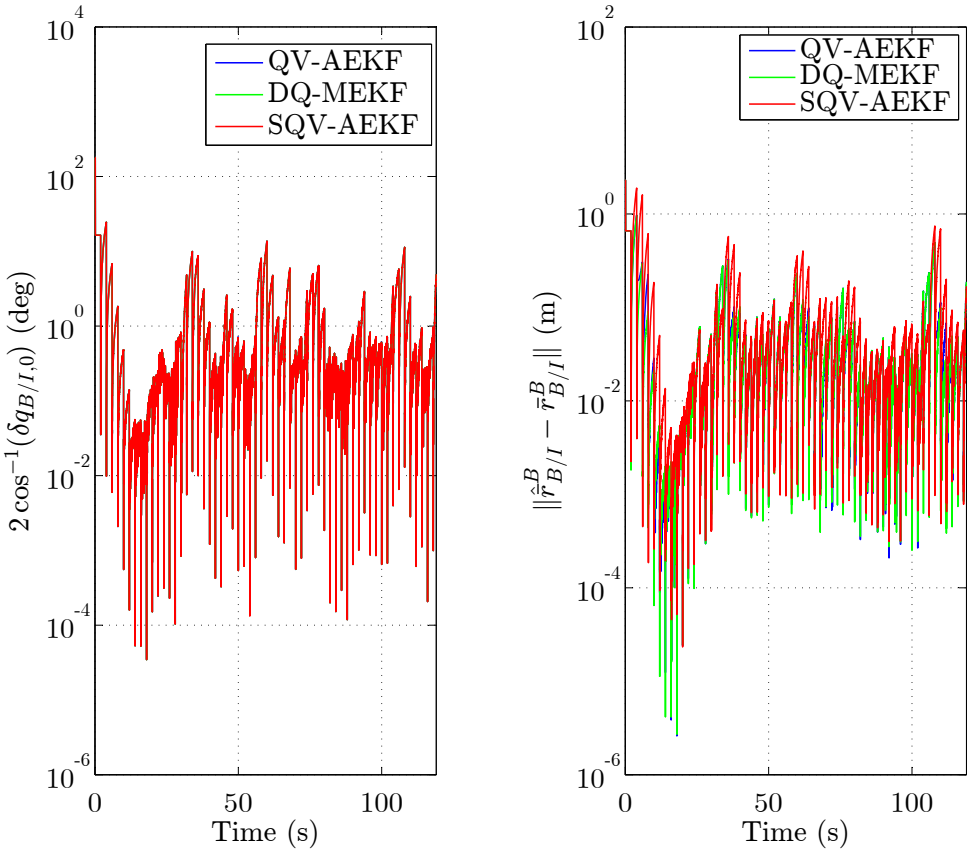

Figure 8. Case 1: pose estimation error (pose measurements at 0.5 Hz).

state is given in Table 6. The same table also shows an a posteriori guess of the initial state based on the measurements. The DQ-MEKF was initialized with the covariance matrices given in Table 7.

Table 6. Case 2: Initial estimate and a posteriori guess of the state.

Variable	Initial Estimate	A Posteriori Guess
$q_{\mathrm{B/I}}(0)$	$[0.6947, -0.0004, 0.0247, 0.7189]^\intercal$ (-)	$[0.7987, -0.0221, -0.0195, 0.6009]^\intercal$ (-)
$\bar{r}^{\mathrm{I}}_{\mathrm{B/I}}(0)$	$[0, 0, 0]^\intercal$ (m)	$[-0.5256, 2.0425, -0.9887]^\intercal$ (m)
$\bar{b}_\omega(0)$	$[-1, 1, 1]^\intercal$ (deg/s)	$[-0.7583, 1.044, 0.6717]^\intercal$ (deg/s)
$\bar{b}_v(0)$	$[0, 0, 0]^\intercal$ (m/s)	$[0, 0, 0]^\intercal$ (m/s)
$\bar{b}_n(0)$	$[0, 0, 0]^\intercal$ (-)	$[0.0251, 0.0160, 0.0005]^\intercal$ (-)

The measured and estimated (i.e., without bias) non-dimensional specific force captured by the accelerometer are plotted in Fig. 10. The difference between the two is the estimated bias of the accelerometer. This estimated bias is higher than the expected bias listed in the accelerometer's datasheet, also given in Table 1. In addition, the estimated bias varies with time when the platform is moving. These two phenomena can be interpreted as the

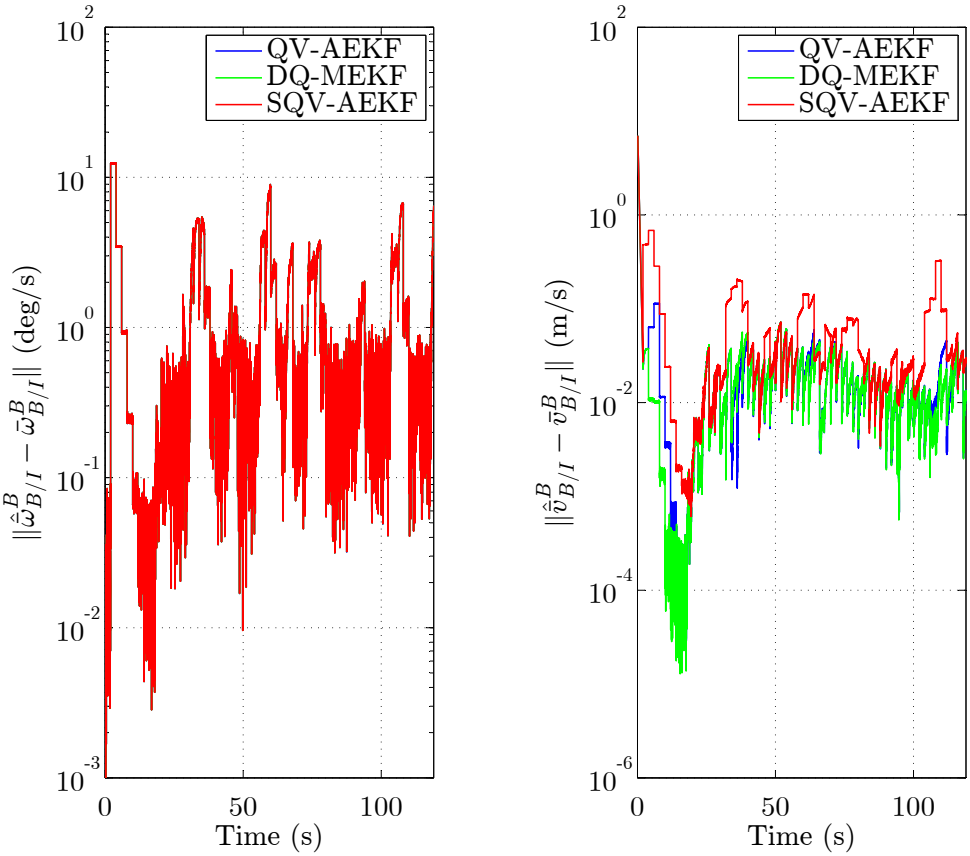

Figure 9. Case 1: angular and linear velocity estimation errors (pose measurements at 0.5 Hz).

DQ-MEKF trying to compensate for errors in the determination of the center of rotation of the upper stage of the 5-DOF platform, errors in the determination of the position of the accelerometer, and errors due to the assumption of zero angular acceleration in Eq. (63).

The measured and estimated (i.e., without bias) angular velocity captured by the rate-gyro are compared in Fig. 11. The difference between the two is the estimated bias of the rate-gyro. This estimated bias is within the expected bias listed in Table 1 and, compared with Fig. 10, does not show any significant variation with time. This is expected, as the errors that effect the bias of the accelerometer do not affect the bias of the rate-gyro.

The estimated pose is compared with the ground truth in Fig. 12 and the pose estimation

Table 7. Case 2: Covariance matrices.

$P_{15\times15}(0)$	$\text{diag}([6.9\times10^{-3}, 6.9\times10^{-3}, 6.9\times10^{-3}, 0.69, 0.69, 0.69, 2\times10^{-6}, 2\times10^{-6}, 2\times10^{-6}, 1\times10^{-9}, 1\times10^{-9}, 1\times10^{-9}, 1.6\times10^{-5}, 1.6\times10^{-5}, 1.6\times10^{-5}])$
$Q_{15\times15}$	$\text{diag}([7\times10^{-7}, 7\times10^{-7}, 7\times10^{-7}, 0, 0, 0, 2\times10^{-6}, 2\times10^{-6}, 2\times10^{-6}, 2\times10^{-7}, 2\times10^{-7}, 2\times10^{-7}])$
$R_{6\times6}$	$\text{diag}([1\times10^{-9}, 1\times10^{-9}, 1\times10^{-9}, 2.5\times10^{-7}, 2.5\times10^{-7}, 2.5\times10^{-7}])$

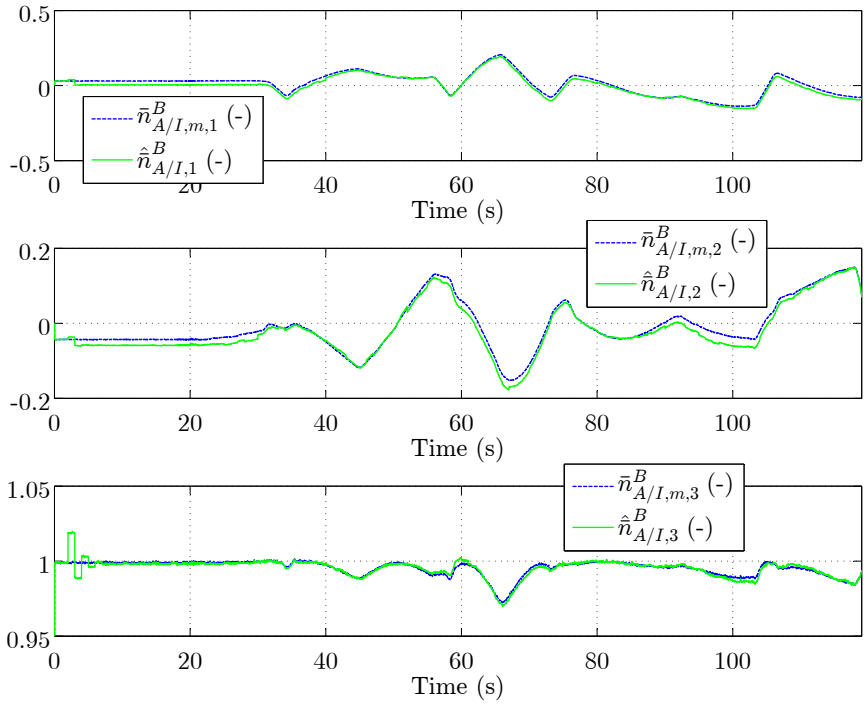

Figure 10. Case 2: estimated and measured non-dimensional specific force.

error is plotted in Fig. 13. After 20 sec, the RMS attitude estimation error is 0.20 deg and the RMS position estimation error is 1.8 cm.

Finally, Fig. 14 shows the linear and angular velocity estimation errors for this case. After 20 sec, the RMS angular velocity estimation error is 0.67 deg/s and the RMS linear velocity estimation error is 3.9 cm/s.

V. Monte-Carlo Simulations

In this section, the DQ-MEKF with no linear and angular velocity measurements is compared with the QV-AEKF and with the SQV-AEKF through 100 Monte-Carlo simulations. A high-fidelity Simulink model of the 5-DOF platform[26] was used to generate pose measurements at different update rates. Measurements of $q_{\mathrm{B/I}}$ were simulated by adding Additive White Gaussian Noise (AWGN) with covariance matrix $1.44 \times 10^{-6} I_{4\times4}$ (-) to the true $q_{\mathrm{B/I}}$, which is available in simulation. After adding the AWGN, the correct norm of the measurements of $q_{\mathrm{B/I}}$ was restored through Eq. (42). Furthermore, measurements of $\overline{r}^{\mathrm{I}}_{\mathrm{B/I}}$ were simulated by adding AWGN with covariance matrix $2.25 \times 10^{-6} I_{3\times3}$ (m^2) to the true $\overline{r}^{\mathrm{I}}_{\mathrm{B/I}}$. Note that in simulation, the exact state is known and can be used as ground truth.

First, the three filters were fed the same measurements of $q_{\mathrm{B/I}}$ and $\overline{r}^{\mathrm{I}}_{\mathrm{B/I}}$ at 10 Hz. The initial estimate of the state used to initialize the three filters is given in Table 8. The same table also shows the true initial state. The three filters were initialized with the covariance

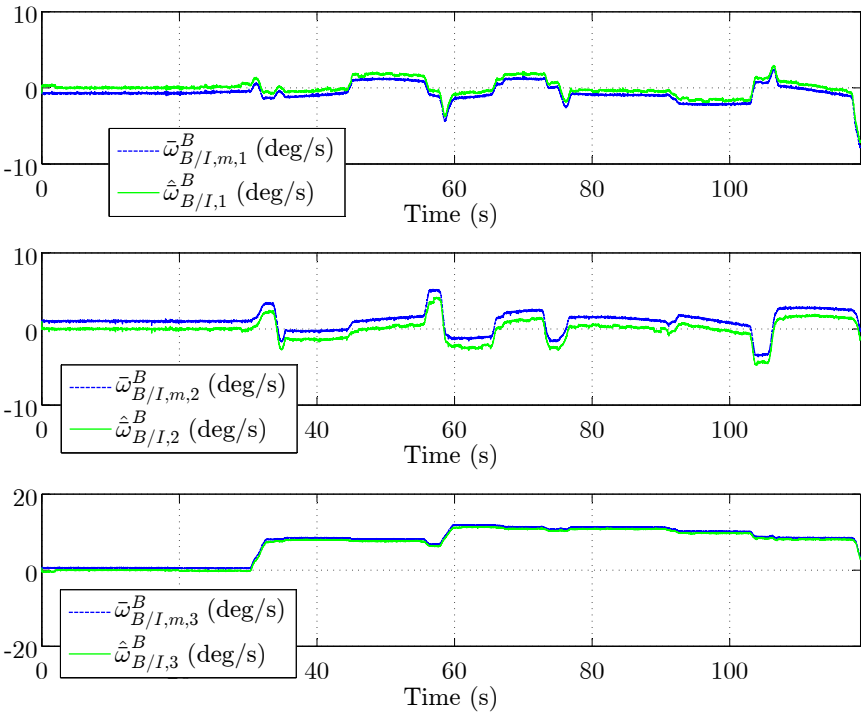

Figure 11. Case 2: estimated and measured angular velocity.

matrices given in Table 3.

Table 8. Monte-Carlo simulation: Initial estimate and true initial state.

Variable	Initial Estimate	True Initial State
$q_{\mathrm{B/I}}(0)$	$[1,0,0,0]^\intercal$ (-)	$[1,0,0,0]^\intercal$ (-)
$\bar{r}^{\mathrm{I}}_{\mathrm{B/I}}(0)$	$[0.1170, 0.9650, -0.0003]^\intercal$ (m)	$[0.1170, 0.9650, -0.0003]^\intercal$ (m)
$\bar{b}_\omega(0)$	$[0,0,0]^\intercal$ (deg/s)	$[0,0,0]^\intercal$ (deg/s)
$\bar{b}_v(0)$	$[0,0,0]^\intercal$ (m/s)	$[0,0,0]^\intercal$ (m/s)

The pose estimated by the DQ-MEKF in one Monte-Carlo run is compared with the true pose in Figure 15 to show the simulated motion of the 5-DOF platform. The motion starts 20 sec after the beginning of the simulation.

The RMS attitude, position, angular velocity, and linear velocity estimation errors after 20 sec obtained in every Monte-Carlo simulation with pose measurements at 10 Hz are shown in Figure 16. As in the experimental results presented in Section IV, the RMS attitude and angular velocity estimation errors obtained with the three filters are the same. Again, this is not surprising since the DQ-MEKF, the QV-AEKF, and the SQV-AEKF represent and update the attitude in the same way and the attitude is independent from the position. Moreover, as in the experimental results presented in Section IV, the RMS position and linear velocity estimation errors obtained with the DQ-MEKF and the QV-AEKF are the

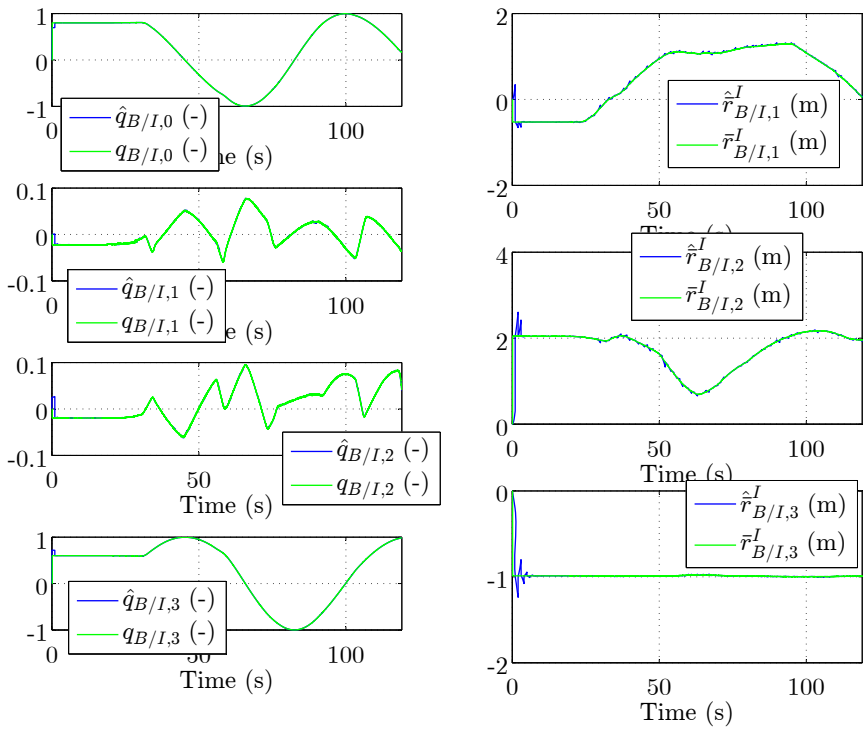

Figure 12. Case 2: estimated and true pose.

same for this measurement update rate. However, compared with the DQ-MEKF and the QV-AEKF, the RMS position estimation error obtained with the SQV-AEKF is slight better, whereas the RMS linear velocity estimation error is clearly worse. Hence, for this update rate, as in Section IV, the DQ-MEKF and the QV-AEKF perform slightly better than the SQV-AEKF. However, since the DQ-MEKF and the QV-AEKF require more states to propagate the state covariance matrix, the SQV-AEKF might be a reasonable choice for a measurement update rate of 10 Hz.

As in Section IV, to compare the filters in a more demanding scenario, the Monte-Carlo simulations were repeated but now with pose measurements at 0.5 Hz. All other parameters were kept the same. As in Figure 16, the RMS attitude and angular velocity estimation errors obtained with the three filters are the same. However, now the SQV-AEKF clearly exhibits the highest RMS position and linear velocity estimation errors. Moreover, as in the experimental results presented in Section IV, for this case, the RMS position and linear velocity estimation errors obtained with the DQ-MEKF are smaller than the ones obtained with the QV-AEKF in every Monte-Carlo run.

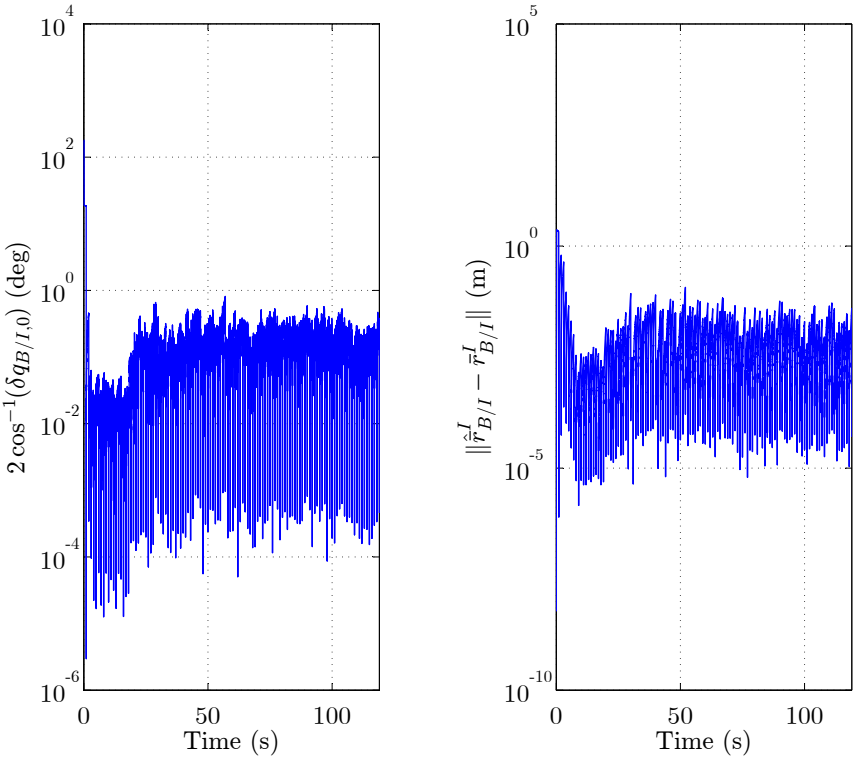

Figure 13. Case 2: pose estimation error.

VI. Conclusion

This paper proposes a Dual Quaternion Multiplicative Extended Kalman Filter (DQ-MEKF) for pose estimation that is an extension of the well-known and widely used Quaternion Multiplicative Extended Kalman Filter (Q-MEKF) for spacecraft attitude estimation. By using the dual quaternion multiplication and the concept of error unit dual quaternion, the two algebraic constraints of unit dual quaternions are automatically satisfied during the measurement update of the DQ-MEKF and the number of states is reduced from eight to six. Three different forms of the DQ-MEKF are presented, each with a different application in mind. Experimental results show that the DQ-MEKF does not encounter singularities and is accurate, precise, and fast enough for operational use. Moreover, when compared with two other EKF formulations, experimental results and Monte-Carlo simulations suggest that the DQ-MEKF might be the best formulation if the measurements are expressed in a different reference frame than the variable to be estimated. This is the case, for example, when one needs the inertial position of a satellite expressed in the body frame, e.g., to implement a control law, but the measurements are expressed in the inertial frame, like the inertial position measurements produced by a GPS. Finally, it should be mentioned that whereas the derivations presented in this paper do not rely on a model of the system dynamics, as they may be hard to model accurately enough, it is relatively straightforward to do so, if desired.

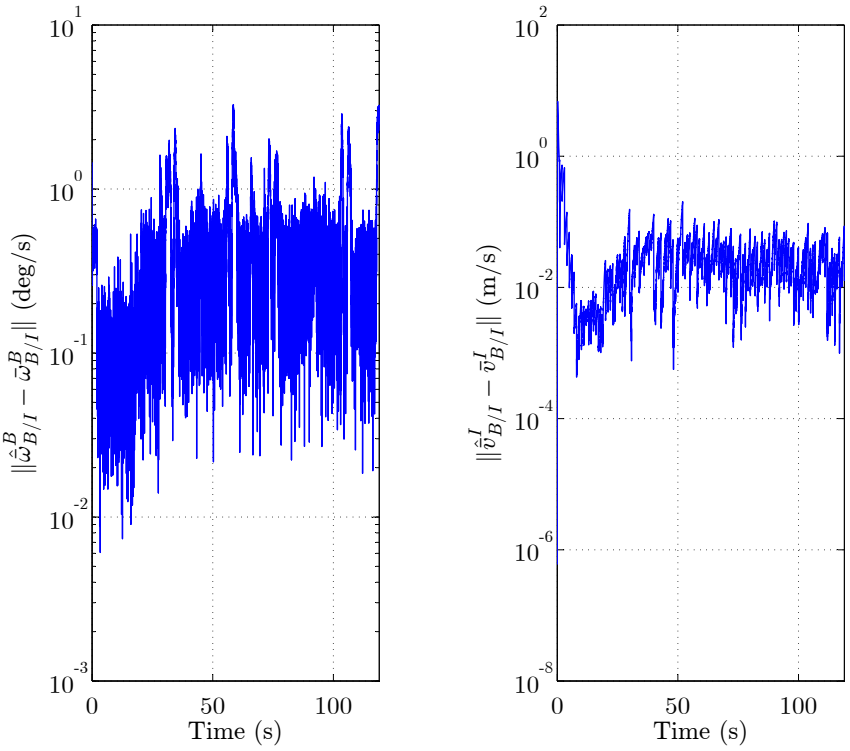

Figure 14. Case 2: angular and linear velocity estimation errors.

Appendix A - Derivation of the QV-AEKF

Instead of representing the pose of a body with respect to the I-frame with a unit dual quaternion (expressed neither in the body frame nor in the I-frame), the attitude and position of a body can be represented separately with a unit quaternion and a translation vector (expressed either in the body frame or in the I-frame). This is the approach taken in Refs. [11–13]. Hereby, an additive EKF based on this representation of the pose is derived for comparison with the DQ-MEKF with no linear and angular velocity measurements. This formulation is referred to as the Quaternion Vector Additive EKF (QV-AEKF).

The linear and angular velocity measurement model is still given by Eq. (25) by separating the real part from the dual part, i.e., $\omega^{\mathrm{B}}_{\mathrm{B/I},m} = \omega^{\mathrm{B}}_{\mathrm{B/I}} + b_\omega + \eta_\omega$ and $v^{\mathrm{B}}_{\mathrm{B/I},m} = v^{\mathrm{B}}_{\mathrm{B/I}} + b_v + \eta_v$, where $E\{\overline{\eta}_\omega\} = 0_{3\times1}$, $E\{\overline{\eta}_v\} = 0_{3\times1}$, $E\{\overline{\eta}_\omega(t)\overline{\eta}^{\mathsf{T}}_\omega(\tau)\} = \overline{Q}_\omega(t)\delta(t-\tau)$, $E\{\overline{\eta}_v(t)\overline{\eta}^{\mathsf{T}}_v(\tau)\} = \overline{Q}_v(t)\delta(t-\tau)$, $\dot{b}_\omega = \eta_{b_\omega}$, $\dot{b}_v = \eta_{b_v}$, $E\left\{\overline{\eta}_{b_\omega}\right\} = 0_{3\times1}$, $E\left\{\overline{\eta}_{b_v}\right\} = 0_{3\times1}$, $E\left\{\overline{\eta}_{b_\omega}(t)\overline{\eta}^{\mathsf{T}}_{b_\omega}(\tau)\right\} = \overline{Q}_{b_\omega}(t)\delta(t-\tau)$, and $E\left\{\overline{\eta}_{b_v}(t)\overline{\eta}^{\mathsf{T}}_{b_v}(\tau)\right\} = \overline{Q}_{b_v}(t)\delta(t-\tau)$.

The state and process noise of the QV-AEKF are initially selected as

$$x_{16} = \begin{bmatrix} [\delta q_{\mathrm{B/I}}]^{\mathsf{T}} & [r^{\mathrm{B}}_{\mathrm{B/I}}]^{\mathsf{T}} & [b_\omega]^{\mathsf{T}} & [b_v]^{\mathsf{T}} \end{bmatrix}^{\mathsf{T}} \in \mathbb{R}^{16} \text{ and } w_{16} = \begin{bmatrix} [\eta_\omega]^{\mathsf{T}} & [\eta_v]^{\mathsf{T}} & [\eta_{b_\omega}]^{\mathsf{T}} & [\eta_{b_v}]^{\mathsf{T}} \end{bmatrix}^{\mathsf{T}} \in \mathbb{R}^{16}.$$

The time derivative of $\delta q_{\mathrm{B/I}}$ is given by the real part of Eq. (37), i.e., $\frac{\mathrm{d}}{\mathrm{d}t}(\delta q_{\mathrm{B/I}}) \approx -\frac{1}{2}\hat{\omega}^{\mathrm{B}}_{\mathrm{B/I}}\delta q_{\mathrm{B/I}} +$

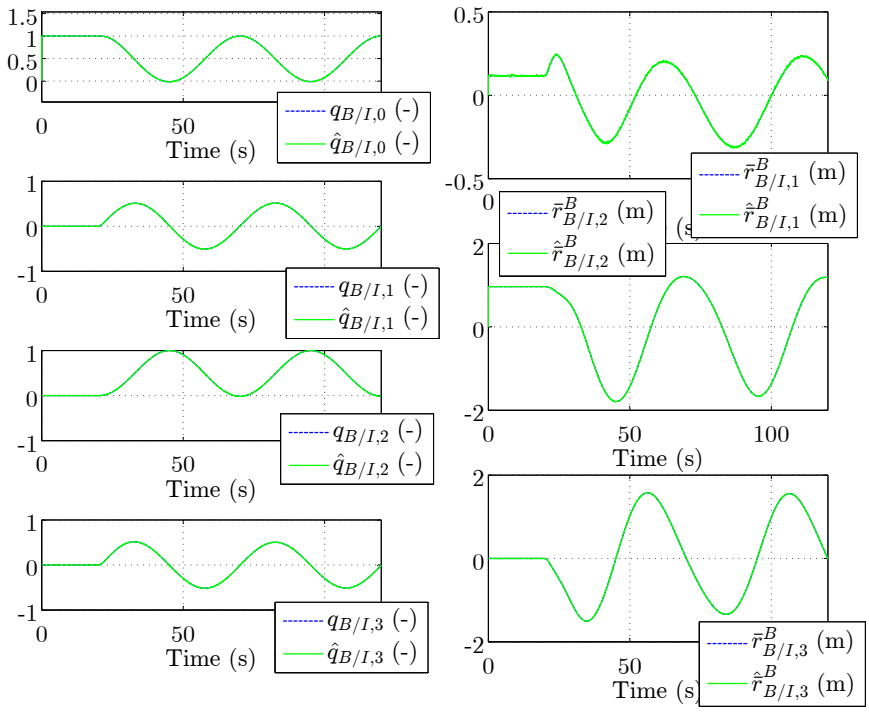

Figure 15. Estimated and true pose for one Monte-Carlo run (pose measurements at 10 Hz).

$\frac{1}{2}\delta q_{\mathrm{B/I}}\hat{\omega}^{\mathrm{B}}_{\mathrm{B/I}} + \frac{1}{2}\delta q_{\mathrm{B/I}}\hat{b}_\omega - \frac{1}{2}\delta q_{\mathrm{B/I}} b_\omega - \frac{1}{2}\delta q_{\mathrm{B/I}}\eta_\omega$, whereas the time derivative of $r^{\mathrm{B}}_{\mathrm{B/I}}$ is given by

$$\frac{\mathrm{d}}{\mathrm{d}t}(r^{\mathrm{B}}_{\mathrm{B/I}}) = v^{\mathrm{B}}_{\mathrm{B/I}} - \omega^{\mathrm{B}}_{\mathrm{B/I}} \times r^{\mathrm{B}}_{\mathrm{B/I}} = (\hat{v}^{\mathrm{B}}_{\mathrm{B/I}} + \hat{b}_v - b_v - \eta_v) - (\hat{\omega}^{\mathrm{B}}_{\mathrm{B/I}} + \hat{b}_\omega - b_\omega - \eta_\omega) \times r^{\mathrm{B}}_{\mathrm{B/I}}. \tag{72}$$

At this point, reduced state and process noise vectors are selected, namely

$$x_{12} = \begin{bmatrix} \overline{\delta q_{\mathrm{B/I}}}^{\mathsf{T}} & (\bar{r}^{\mathrm{B}}_{\mathrm{B/I}})^{\mathsf{T}} & \bar{b}_\omega^{\mathsf{T}} & \bar{b}_v^{\mathsf{T}} \end{bmatrix}^{\mathsf{T}} \in \mathbb{R}^{12} \text{ and } w_{12} = \begin{bmatrix} \bar{\eta}_\omega^{\mathsf{T}} & \bar{\eta}_v^{\mathsf{T}} & \bar{\eta}_{b_\omega}^{\mathsf{T}} & \bar{\eta}_{b_v}^{\mathsf{T}} \end{bmatrix}^{\mathsf{T}} \in \mathbb{R}^{12}.$$

The state equations of the QV-AEKF are then given by

$$f_{12}(x_{12}(t), t) = \begin{bmatrix} \overline{-\frac{1}{2}\hat{\omega}^{\mathrm{B}}_{\mathrm{B/I}}\delta q_{\mathrm{B/I}} + \frac{1}{2}\delta q_{\mathrm{B/I}}\hat{\omega}^{\mathrm{B}}_{\mathrm{B/I}} + \frac{1}{2}\delta q_{\mathrm{B/I}}\hat{b}_\omega - \frac{1}{2}\delta q_{\mathrm{B/I}} b_\omega} \\ (\hat{v}^{\mathrm{B}}_{\mathrm{B/I}} + \hat{b}_v - b_v) - (\hat{\omega}^{\mathrm{B}}_{\mathrm{B/I}} + \hat{b}_\omega - b_\omega) \times r^{\mathrm{B}}_{\mathrm{B/I}} \\ 0_{3\times 1} \\ 0_{3\times 1} \end{bmatrix}, \tag{73}$$

$$g_{16\times 16}(x_{16}(t), t) = \begin{bmatrix} -\frac{1}{2}[\widetilde{\delta q_{\mathrm{B/I}}}] & 0_{3\times 3} & 0_{3\times 3} & 0_{3\times 3} \\ -\overline{r^{\mathrm{B}}_{\mathrm{B/I}}}^{\times} & -I_{3\times 3} & 0_{3\times 3} & 0_{3\times 3} \\ 0_{3\times 3} & 0_{3\times 3} & I_{3\times 3} & 0_{3\times 3} \\ 0_{3\times 3} & 0_{3\times 3} & 0_{3\times 3} & I_{3\times 3} \end{bmatrix}. \tag{74}$$

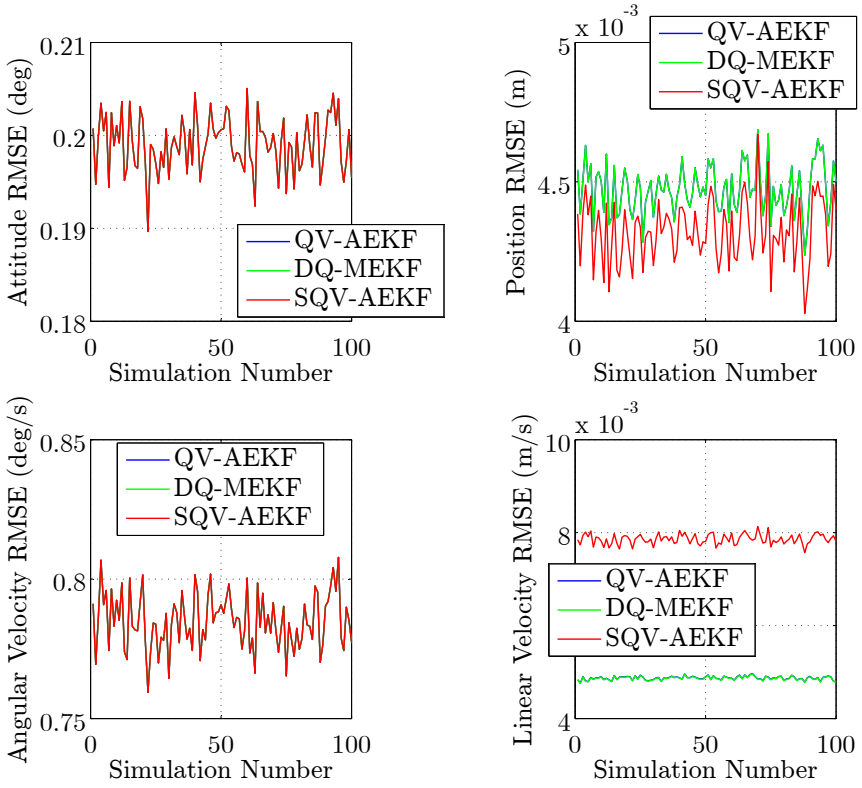

Figure 16. State estimation Root-Mean-Square Errors (RMSE) after 20 sec obtained in every Monte-Carlo simulation (pose measurements at 10 Hz).

By replacing $\delta q_{\mathrm{B/I},0}$ through Eq. (17) in Eqs. (73) and (74) and using Eq. (5), $F_{12\times12}(t)$ and $G_{12\times12}(t)$ can be determined to be, respectively,

$$\begin{bmatrix} -\overline{\hat{\omega}^{\mathrm{B}}_{\mathrm{B/I}}}^{\times} & 0_{3\times3} & -\frac{1}{2}I_{3\times3} & 0_{3\times3} \\ 0_{3\times3} & -\overline{\hat{\omega}^{\mathrm{B}}_{\mathrm{B/I}}}^{\times} & -\overline{\hat{r}^{\mathrm{B}}_{\mathrm{B/I}}}^{\times} & -I_{3\times3} \\ 0_{3\times3} & 0_{3\times3} & 0_{3\times3} & 0_{3\times3} \\ 0_{3\times3} & 0_{3\times3} & 0_{3\times3} & 0_{3\times3} \end{bmatrix}, \begin{bmatrix} -\frac{1}{2}I_{3\times3} & 0_{3\times3} & 0_{3\times3} & 0_{3\times3} \\ -\overline{\hat{r}^{\mathrm{B}}_{\mathrm{B/I}}}^{\times} & -I_{3\times3} & 0_{3\times3} & 0_{3\times3} \\ 0_{3\times3} & 0_{3\times3} & I_{3\times3} & 0_{3\times3} \\ 0_{3\times3} & 0_{3\times3} & 0_{3\times3} & I_{3\times3} \end{bmatrix}. \tag{75}$$

VI..1. Time Update

For the time update of the QV-AEKF, $\hat{q}_{\mathrm{B/I}}$, $\hat{r}^{\mathrm{B}}_{\mathrm{B/I}}$, $\hat{\omega}^{\mathrm{B}}_{\mathrm{B/I}}$, $\hat{v}^{\mathrm{B}}_{\mathrm{B/I}}$, $\hat{b}_\omega$, and $\hat{b}_v$ are propagated using the real part of Eq. (31), i.e., $\frac{\mathrm{d}}{\mathrm{d}t}(\hat{q}_{\mathrm{B/I}}) \approx \frac{1}{2}\hat{q}_{\mathrm{B/I}}\hat{\omega}^{\mathrm{B}}_{\mathrm{B/I}}$, $\frac{\mathrm{d}}{\mathrm{d}t}(\hat{r}^{\mathrm{B}}_{\mathrm{B/I}}) \approx \hat{v}^{\mathrm{B}}_{\mathrm{B/I}} - \hat{\omega}^{\mathrm{B}}_{\mathrm{B/I}} \times \hat{r}^{\mathrm{B}}_{\mathrm{B/I}}$, $\hat{\omega}^{\mathrm{B}}_{\mathrm{B/I}} = \omega^{\mathrm{B}}_{\mathrm{B/I},m} - \hat{b}_\omega$, $\hat{v}^{\mathrm{B}}_{\mathrm{B/I}} = v^{\mathrm{B}}_{\mathrm{B/I},m} - \hat{b}_v$, $\frac{\mathrm{d}}{\mathrm{d}t}(\hat{b}_\omega) = 0$, and $\frac{\mathrm{d}}{\mathrm{d}t}(\hat{b}_v) = 0$, respectively, given $\hat{q}_{\mathrm{B/I}}(t_0)$, $\hat{r}^{\mathrm{B}}_{\mathrm{B/I}}(t_0)$, $\hat{b}_\omega(t_0)$, and $\hat{b}_v(t_0)$.

Numerical errors in the propagation of $\hat{q}_{\mathrm{B/I}}$ may result in $\hat{q}_{\mathrm{B/I}}$ violating the unit norm constraint. Hence, after each integration step, this algebraic constraint is enforced by using Eq. (42).

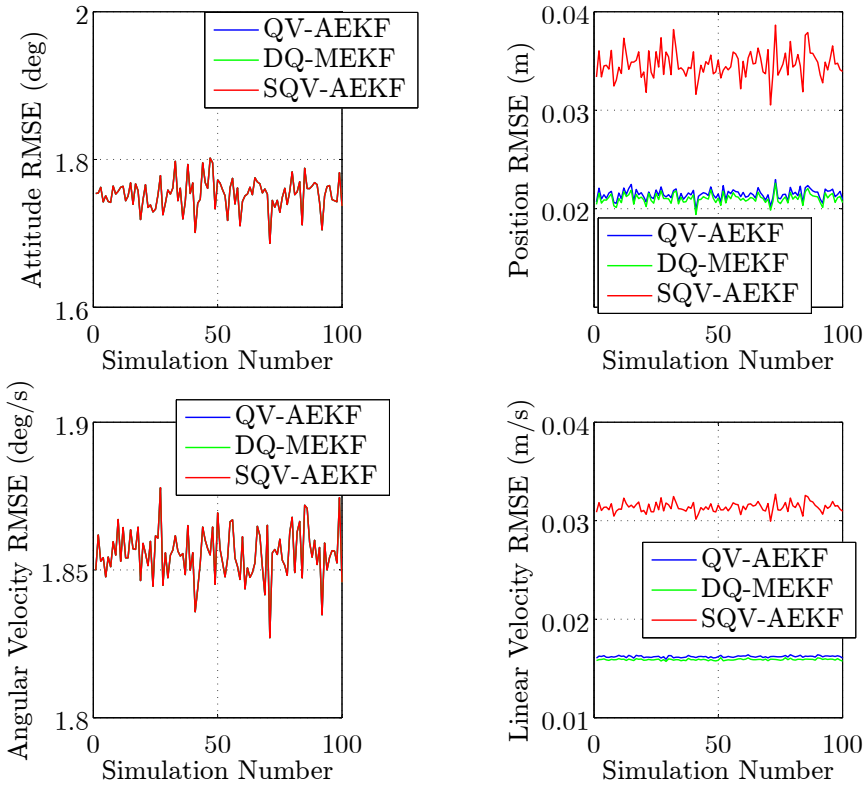

Figure 17. State estimation Root-Mean-Square Errors (RMSE) after 20 sec obtained in every Monte-Carlo simulation (pose measurements at 0.5 Hz).

As for the covariance matrix of x_{12},

$$P_{12\times12}(t) \triangleq E\left\{\left(\begin{bmatrix}\overline{\delta q_{\mathrm{B/I}}}(t)\\ \overline{r}^{\mathrm{B}}_{\mathrm{B/I}}(t)\\ \overline{b}_{\omega}(t)\\ \overline{b}_{v}(t)\end{bmatrix}-\begin{bmatrix}0_{3\times1}\\ \hat{\overline{r}}^{\mathrm{B}}_{\mathrm{B/I}}(t)\\ \hat{\overline{b}}_{\omega}(t)\\ \hat{\overline{b}}_{v}(t)\end{bmatrix}\right)\left(\begin{bmatrix}\overline{\delta q_{\mathrm{B/I}}}(t)\\ \overline{r}^{\mathrm{B}}_{\mathrm{B/I}}(t)\\ \overline{b}_{\omega}(t)\\ \overline{b}_{v}(t)\end{bmatrix}-\begin{bmatrix}0_{3\times1}\\ \hat{\overline{r}}^{\mathrm{B}}_{\mathrm{B/I}}(t)\\ \hat{\overline{b}}_{\omega}(t)\\ \hat{\overline{b}}_{v}(t)\end{bmatrix}\right)^{\mathsf{T}}\right\}, \tag{76}$$

it is propagated according to Eq. (4) given $P_{12\times12}(t_0)$ and where

$$Q_{12\times12}(t) = \begin{bmatrix}\overline{Q}_{\omega}(t) & 0_{3\times3} & 0_{3\times3} & 0_{3\times3}\\ 0_{3\times3} & \overline{Q}_{v}(t) & 0_{3\times3} & 0_{3\times3}\\ 0_{3\times3} & 0_{3\times3} & \overline{Q}_{b_{\omega}}(t) & 0_{3\times3}\\ 0_{3\times3} & 0_{3\times3} & 0_{3\times3} & \overline{Q}_{b_{v}}(t)\end{bmatrix}. \tag{77}$$

VI..2. Measurement Update

For direct comparison with the DQ-MEKF with output equation given by Eq. (51), it is assumed that the QV-AEKF is fed measurements of $q_{\mathrm{B/I}}$ and $r^{\mathrm{I}}_{\mathrm{B/I}}$. The output equation of

the QV-AEKF is defined as

$$\begin{bmatrix} \overline{(\hat{q}^{-}_{\mathrm{B/I}}(t_k))^* q_{\mathrm{B/I},m}(t_k)} \\ \overline{r^{\mathrm{I}}_{\mathrm{B/I},m}(t_k)} \end{bmatrix} = \begin{bmatrix} \overline{\delta q_{\mathrm{B/I}}(t_k)} \\ \overline{\hat{q}_{\mathrm{B/I}}(t_k)\delta q_{\mathrm{B/I}}(t_k) r^{\mathrm{B}}_{\mathrm{B/I}}(t_k)\delta q^*_{\mathrm{B/I}}(t_k)\hat{q}^*_{\mathrm{B/I}}(t_k)} \end{bmatrix} + v_6(t_k). \tag{78}$$

Hence, using Eq. (11) to calculate the measurement sensitivity matrix yields

$$H_{6\times 12}(t_k) = \begin{bmatrix} I_{3\times 3} & 0_{3\times 3} & 0_{3\times 3} & 0_{3\times 3} \\ -2R\left((\hat{q}^{-}_{\mathrm{B/I}})^*\right)\overline{\hat{r}^{\mathrm{B},-}_{\mathrm{B/I}}}^{\times} & R\left((\hat{q}^{-}_{\mathrm{B/I}})^*\right) & 0_{3\times 3} & 0_{3\times 3}. \end{bmatrix}. \tag{79}$$

In summary, for the measurement update of the QV-AEKF, the Kalman gain is calculated from Eq. (10), whereas the optimal Kalman state update is calculated from Eq. (8) as

$$\Delta^\star \hat{x}_{12}(t_k) \triangleq \begin{bmatrix} \Delta^\star \overline{\delta\hat{q}_{\mathrm{B/I}}}(t_k) \\ \Delta^\star \overline{\hat{r}}^{\mathrm{B}}_{\mathrm{B/I}}(t_k) \\ \Delta^\star \overline{\hat{b}}_{\omega}(t_k) \\ \Delta^\star \overline{\hat{b}}_{v}(t_k) \end{bmatrix} = K_{12\times 6}(t_k) \left(\begin{bmatrix} \overline{(\hat{q}^{-}_{\mathrm{B/I}}(t_k))^* q_{\mathrm{B/I},m}(t_k)} \\ \overline{r^{\mathrm{I}}_{\mathrm{B/I},m}(t_k)} \end{bmatrix} - \begin{bmatrix} 0_{3\times 3} \\ \overline{\hat{r}^{\mathrm{I},-}_{\mathrm{B/I}}(t_k)} \end{bmatrix} \right).$$

The estimate of the state at time t_k after the measurement is then calculated from $\hat{q}^{+}_{\mathrm{B/I}}(t_k) = \hat{q}^{-}_{\mathrm{B/I}}(t_k)\Delta^\star\delta\hat{q}_{\mathrm{B/I}}(t_k)$, $\overline{\hat{b}}^{+}_{\omega}(t_k) = \overline{\hat{b}}^{-}_{\omega}(t_k) + \Delta^\star\overline{\hat{b}}_{\omega}(t_k)$, $\overline{\hat{b}}^{+}_{v}(t_k) = \overline{\hat{b}}^{-}_{v}(t_k) + \Delta^\star\overline{\hat{b}}_{v}(t_k)$, and

$$\overline{\hat{r}}^{\mathrm{B},+}_{\mathrm{B/I}}(t_k) = \overline{\hat{r}}^{\mathrm{B},-}_{\mathrm{B/I}}(t_k) + \Delta^\star\overline{\hat{r}}^{\mathrm{B}}_{\mathrm{B/I}}, \tag{80}$$

where $\Delta^\star\delta\hat{q}_{\mathrm{B/I}}$ is defined as the unit quaternion

$$\left(\sqrt{1-\|\Delta^\star\overline{\delta\hat{q}_{\mathrm{B/I}}}\|^2}, \Delta^\star\overline{\delta\hat{q}_{\mathrm{B/I}}}\right), \text{ or } \left(\frac{1}{\sqrt{1+\|\Delta^\star\overline{\delta\hat{q}_{\mathrm{B/I}}}\|^2}}, \frac{\Delta^\star\overline{\delta\hat{q}_{\mathrm{B/I}}}}{\sqrt{1+\|\Delta^\star\overline{\delta\hat{q}_{\mathrm{B/I}}}\|^2}}\right) \tag{81}$$

if the norm of $\Delta^\star\overline{\delta\hat{q}_{\mathrm{B/I}}}$ is larger than one. Note that whereas the optimal Kalman state update is added in Eq. (80), it is multiplied in Eq. (48). Finally, the covariance matrix of the state immediately after the measurement at t_k is computed from Eq. (13).

As before, when position and attitude measurements are available, but linear and angular velocity measurements are not, estimates of $\omega^{\mathrm{B}}_{\mathrm{B/I}}$ and $v^{\mathrm{B}}_{\mathrm{B/I}}$ can be determined by setting $\omega^{\mathrm{B}}_{\mathrm{B/I},m}$, $v^{\mathrm{B}}_{\mathrm{B/I},m}$, $\overline{Q}_{\omega}$, and $\overline{Q}_{v}$ to zero, and by increasing $\overline{Q}_{b_\omega}$ and $\overline{Q}_{b_v}$ if necessary.

Appendix B - Derivation of the SQV-AEKF

Whereas the states of the DQ-MEKF and of the QV-AEKF include both the attitude and position of the body, the traditional approach to estimating the pose consists of developing separate estimators for the attitude and for the position.[10] To compare this traditional approach to the DQ-MEKF and to the QV-AEKF, the QV-AEKF is split here into two additive EKFs, one for the attitude and another one for the position. This alternative formulation is referred to as the Split Quaternion Vector Additive EKF (SQV-AEKF).

VI.A. Attitude Estimation with the SQV-AEKF

As in the QV-AEKF, the angular velocity measurement model is given by $\omega^{\mathrm{B}}_{\mathrm{B/I},m} = \omega^{\mathrm{B}}_{\mathrm{B/I}} + b_\omega + \eta_\omega$, where $E\left\{\overline{\eta}_\omega\right\} = 0_{3\times1}$, $E\left\{\overline{\eta}_\omega(t)\overline{\eta}^{\mathsf{T}}_\omega(\tau)\right\} = \overline{Q}_\omega(t)\delta(t-\tau)$, $\dot{b}_\omega = \eta_{b_\omega}$, $E\left\{\overline{\eta}_{b_\omega}\right\} = 0_{3\times1}$, and $E\left\{\overline{\eta}_{b_\omega}(t)\overline{\eta}^{\mathsf{T}}_{b_\omega}(\tau)\right\} = \overline{Q}_{b_\omega}(t)\delta(t-\tau)$.

The state and process noise of the attitude part of the SQV-AEKF are initially selected as

$$x_8=[[\delta q_{\mathrm{B/I}}]^{\mathsf{T}}\ [b_\omega]^{\mathsf{T}}]^{\mathsf{T}} \in \mathbb{R}^8 \text{ and } w_8=[[\eta_\omega]^{\mathsf{T}}\ [\eta_{b_\omega}]^{\mathsf{T}}]^{\mathsf{T}} \in \mathbb{R}^8.$$

As in the QV-AEKF, the time derivative of $\delta q_{\mathrm{B/I}}$ is given by $\frac{\mathrm{d}}{\mathrm{d}t}(\delta q_{\mathrm{B/I}}) \approx -\frac{1}{2}\hat{\omega}^{\mathrm{B}}_{\mathrm{B/I}}\delta q_{\mathrm{B/I}} + \frac{1}{2}\delta q_{\mathrm{B/I}}\hat{\omega}^{\mathrm{B}}_{\mathrm{B/I}} + \frac{1}{2}\delta q_{\mathrm{B/I}}\hat{b}_\omega - \frac{1}{2}\delta q_{\mathrm{B/I}}b_\omega - \frac{1}{2}\delta q_{\mathrm{B/I}}\eta_\omega$.

At this point, reduced state and process noise vectors are selected, namely

$$x_6 = [\overline{\delta q_{\mathrm{B/I}}}^{\mathsf{T}}\ \overline{b}^{\mathsf{T}}_\omega]^{\mathsf{T}} \in \mathbb{R}^6 \text{ and } w_6 = [\overline{\eta}^{\mathsf{T}}_\omega\ \overline{\eta}^{\mathsf{T}}_{b_\omega}]^{\mathsf{T}} \in \mathbb{R}^6.$$

The state equations of the attitude part of the SQV-AEKF are then defined by $f_6(x_6(t),t)$ and $g_{6\times6}(x_6(t),t)$, which are given by, respectively,

$$\begin{bmatrix} \overline{-\frac{1}{2}\hat{\omega}^{\mathrm{B}}_{\mathrm{B/I}}\delta q_{\mathrm{B/I}} + \frac{1}{2}\delta q_{\mathrm{B/I}}\hat{\omega}^{\mathrm{B}}_{\mathrm{B/I}} + \frac{1}{2}\delta q_{\mathrm{B/I}}\hat{b}_\omega - \frac{1}{2}\delta q_{\mathrm{B/I}}b_\omega} \\ 0_{3\times1} \end{bmatrix}, \begin{bmatrix} -\frac{1}{2}\widetilde{[\delta q_{\mathrm{B/I}}]} & 0_{3\times3} \\ 0_{3\times3} & I_{3\times3} \end{bmatrix}. \tag{82}$$

By replacing $\delta q_{\mathrm{B/I},0}$ through Eq. (17) in $f_6(x_6(t),t)$ and $g_{6\times6}(x_6(t),t)$ and using Eq. (5), $F_{6\times6}(t)$ and $G_{6\times6}(t)$ can be determined to be

$$F_{6\times6}(t) = \begin{bmatrix} -\overline{\hat{\omega}^{\mathrm{B}}_{\mathrm{B/I}}}^{\times} & -\frac{1}{2}I_{3\times3} \\ 0_{3\times3} & 0_{3\times3} \end{bmatrix},\ G_{6\times6}(t) = \begin{bmatrix} -\frac{1}{2}I_{3\times3} & 0_{3\times3} \\ 0_{3\times3} & I_{3\times3} \end{bmatrix}. \tag{83}$$

VI.A.1. Time Update

For the time update of the attitude part of the SQV-AEKF, $\hat{q}_{\mathrm{B/I}}$, $\hat{\omega}^{\mathrm{B}}_{\mathrm{B/I}}$, and $\hat{b}_\omega$ are propagated using $\frac{\mathrm{d}}{\mathrm{d}t}(\hat{q}_{\mathrm{B/I}}) \approx \frac{1}{2}\hat{q}_{\mathrm{B/I}}\hat{\omega}^{\mathrm{B}}_{\mathrm{B/I}}$, $\hat{\omega}^{\mathrm{B}}_{\mathrm{B/I}} = \omega^{\mathrm{B}}_{\mathrm{B/I},m} - \hat{b}_\omega$, and $\frac{\mathrm{d}}{\mathrm{d}t}(\hat{b}_\omega) = 0$, respectively, given $\hat{q}_{\mathrm{B/I}}(t_0)$ and

$\hat{b}_\omega(t_0)$. After each integration step, the unit norm constraint for $\hat{q}_{\mathrm{B/I}}$ is enforced using Eq. (42).

As for the covariance matrix of x_6,

$$P_{6\times6}(t) \triangleq E\left\{\left(\begin{bmatrix}\overline{\delta q_{\mathrm{B/I}}}(t)\\ \overline{b}_\omega(t)\end{bmatrix} - \begin{bmatrix}0_{3\times1}\\ \hat{\overline{b}}_\omega(t)\end{bmatrix}\right)\left(\begin{bmatrix}\overline{\delta q_{\mathrm{B/I}}}(t)\\ \overline{b}_\omega(t)\end{bmatrix} - \begin{bmatrix}0_{3\times1}\\ \hat{\overline{b}}_\omega(t)\end{bmatrix}\right)^{\mathsf{T}}\right\}, \tag{84}$$

it is propagated according to Eq. (4) given $P_{6\times6}(t_0)$ and where

$$Q_{6\times6}(t) = \begin{bmatrix}\overline{Q}_\omega(t) & 0_{3\times3}\\ 0_{3\times3} & \overline{Q}_{b_\omega}(t)\end{bmatrix}. \tag{85}$$

VI.A.2. Measurement Update

It is assumed that the attitude part of the SQV-AEKF is fed measurements of $q_{\mathrm{B/I}}$ (whereas the position part of the SQV-AEKF is fed measurements of $r^{\mathrm{I}}_{\mathrm{B/I}}$). Hence, the output equation of the attitude part of the SQV-AEKF is given by

$$\overline{(\hat{q}^-_{\mathrm{B/I}}(t_k))^* q_{\mathrm{B/I},m}(t_k)} = \overline{\delta q_{\mathrm{B/I}}(t_k)} + v_3(t_k). \tag{86}$$

Hence, using Eq. (11) to calculate the measurement sensitivity matrix yields

$$H_{3\times6}(t_k) = \left[I_{3\times3}\ 0_{3\times3}\right]. \tag{87}$$

In summary, for the measurement update of the attitude part of the SQV-AEKF, the Kalman gain is calculated from Eq. (10), whereas the optimal Kalman state update is calculated from Eq. (8) as

$$\Delta^\star \hat{x}_6(t_k) \triangleq \begin{bmatrix}\Delta^\star\overline{\delta\hat{q}_{\mathrm{B/I}}}(t_k)\\ \Delta^\star\hat{\overline{b}}_\omega(t_k)\end{bmatrix} = K_{6\times3}(t_k)(\overline{(\hat{q}^-_{\mathrm{B/I}}(t_k))^* q_{\mathrm{B/I},m}(t_k)} - 0_{3\times3}). \tag{88}$$

The estimate of the state at time t_k after the measurement is then calculated from $\hat{q}^+_{\mathrm{B/I}}(t_k) = \hat{q}^-_{\mathrm{B/I}}(t_k)\Delta^\star\delta\hat{q}_{\mathrm{B/I}}(t_k)$ and $\hat{\overline{b}}^+_\omega(t_k) = \hat{\overline{b}}^-_\omega(t_k) + \Delta^\star\hat{\overline{b}}_\omega(t_k)$, where $\Delta^\star\delta\hat{q}_{\mathrm{B/I}}$ is the unit quaternion defined in Eq. (81). Finally, the covariance matrix of the state immediately after the measurement at t_k is computed from Eq. (13).

As before, when attitude measurements are available, but angular velocity measurements are not, estimates of $\omega^{\mathrm{B}}_{\mathrm{B/I}}$ can be determined by setting $\omega^{\mathrm{B}}_{\mathrm{B/I},m}$ and $\overline{Q}_\omega$ to zero, and by increasing $\overline{Q}_{b_\omega}$ if necessary.

VI.B. Position Estimation with the SQV-AEKF

As in the QV-AEKF, the linear velocity measurement model is given by $v^{\mathrm{B}}_{\mathrm{B/I},m} = v^{\mathrm{B}}_{\mathrm{B/I}} + b_v + \eta_v$, where $E\{\overline{\eta}_v\} = 0_{3\times1}$, $E\{\overline{\eta}_v(t)\overline{\eta}_v^{\mathsf{T}}(\tau)\} = \overline{Q}_v(t)\delta(t-\tau)$, $\dot{b}_v = \eta_{b_v}$, $E\left\{\overline{\eta}_{b_v}\right\} = 0_{3\times1}$, and $E\left\{\overline{\eta}_{b_v}(t)\overline{\eta}_{b_v}^{\mathsf{T}}(\tau)\right\} = \overline{Q}_{b_v}(t)\delta(t-\tau)$.

The state and process noise of the position part of the SQV-AEKF are selected as

$$x_6 = [(\overline{r}^{\mathrm{B}}_{\mathrm{B/I}})^{\mathsf{T}}\ \overline{b}_v^{\mathsf{T}}]^{\mathsf{T}} \in \mathbb{R}^6 \text{ and } w_6 = [\overline{\eta}_v^{\mathsf{T}}\ \overline{\eta}_{b_v}^{\mathsf{T}}]^{\mathsf{T}} \in \mathbb{R}^6.$$

The time derivative of $r^{\mathrm{B}}_{\mathrm{B/I}}$ is given by Eq. (72). Hence, the state equations of the position part of the SQV-AEKF are defined by $f_6(x_6(t),t)$ and $g_{6\times6}(x_6(t),t)$, which are given by, respectively,

$$\begin{bmatrix} \overline{(\hat{v}^{\mathrm{B}}_{\mathrm{B/I}} + \hat{b}_v - b_v) - (\hat{\omega}^{\mathrm{B}}_{\mathrm{B/I}} + \hat{b}_\omega - b_\omega) \times r^{\mathrm{B}}_{\mathrm{B/I}}} \\ 0_{3\times1} \end{bmatrix}, \qquad \begin{bmatrix} -I_{3\times3} & 0_{3\times3} \\ 0_{3\times3} & I_{3\times3} \end{bmatrix}. \tag{89}$$

Using Eq. (5), $F_{6\times6}(t)$ and $G_{6\times6}(t)$ can be determined to be

$$F_{6\times6}(t) = \begin{bmatrix} -\overline{\hat{\omega}^{\mathrm{B}}_{\mathrm{B/I}}}^{\times} & -I_{3\times3} \\ 0_{3\times3} & 0_{3\times3} \end{bmatrix}, \qquad G_{6\times6}(t) = \begin{bmatrix} -I_{3\times3} & 0_{3\times3} \\ 0_{3\times3} & I_{3\times3} \end{bmatrix}. \tag{90}$$

Note that $F_{6\times6}(t)$ is a function of $\overline{\hat{\omega}^{\mathrm{B}}_{\mathrm{B/I}}}$, which is an output of the attitude part of the SQV-AEKF.

VI.B.1. Time Update

For the time update of the position part of the SQV-AEKF, $\hat{r}^{\mathrm{B}}_{\mathrm{B/I}}$, $\hat{v}^{\mathrm{B}}_{\mathrm{B/I}}$, and $\hat{b}_v$ are propagated using $\frac{\mathrm{d}}{\mathrm{d}t}(\hat{r}^{\mathrm{B}}_{\mathrm{B/I}}) \approx \hat{v}^{\mathrm{B}}_{\mathrm{B/I}} - \hat{\omega}^{\mathrm{B}}_{\mathrm{B/I}} \times \hat{r}^{\mathrm{B}}_{\mathrm{B/I}}$, $\hat{v}^{\mathrm{B}}_{\mathrm{B/I}} = v^{\mathrm{B}}_{\mathrm{B/I},m} - \hat{b}_v$, and $\frac{\mathrm{d}}{\mathrm{d}t}(\hat{b}_v) = 0$, respectively, given $\hat{r}^{\mathrm{B}}_{\mathrm{B/I}}(t_0)$ and $\hat{b}_v(t_0)$. Note that $\frac{\mathrm{d}}{\mathrm{d}t}(\hat{r}^{\mathrm{B}}_{\mathrm{B/I}})$ is a function of $\hat{\omega}^{\mathrm{B}}_{\mathrm{B/I}}$, which is an output of the attitude part of the SQV-AEKF.

As for the covariance matrix of x_6,

$$P_{6\times6}(t) \triangleq E\left\{ \left(\begin{bmatrix} \overline{r}^{\mathrm{B}}_{\mathrm{B/I}}(t) \\ \overline{b}_v(t) \end{bmatrix} - \begin{bmatrix} \hat{\overline{r}}^{\mathrm{B}}_{\mathrm{B/I}}(t) \\ \hat{\overline{b}}_v(t) \end{bmatrix} \right) \left(\begin{bmatrix} \overline{r}^{\mathrm{B}}_{\mathrm{B/I}}(t) \\ \overline{b}_v(t) \end{bmatrix} - \begin{bmatrix} \hat{\overline{r}}^{\mathrm{B}}_{\mathrm{B/I}}(t) \\ \hat{\overline{b}}_v(t) \end{bmatrix} \right)^{\mathsf{T}} \right\}, \tag{91}$$

it is propagated according to Eq. (4) given $P_{12\times12}(t_0)$ and where

$$Q_{12\times12}(t) = \begin{bmatrix} \overline{Q}_v(t) & 0_{3\times3} \\ 0_{3\times3} & \overline{Q}_{b_v}(t) \end{bmatrix}. \tag{92}$$

VI.B.2. Measurement Update

It is assumed that the position part of the SQV-AEKF is fed measurements of $r^{\mathrm{I}}_{\mathrm{B/I}}$ (whereas the attitude part of the SQV-AEKF is fed measurements of $q_{\mathrm{B/I}}$). Hence, the output equation of the position part of the SQV-AEKF is given by

$$\overline{r}^{\mathrm{I}}_{\mathrm{B/I},m}(t_k) = \overline{\hat{q}_{\mathrm{B/I}}(t_k)\delta q_{\mathrm{B/I}}(t_k) r^{\mathrm{B}}_{\mathrm{B/I}}(t_k)\delta q^{*}_{\mathrm{B/I}}(t_k)\hat{q}^{*}_{\mathrm{B/I}}(t_k)} + v_3(t_k). \tag{93}$$

Calculating the measurement sensitivity matrix using Eq. (11) yields

$$H_{3\times 6}(t_k) = \left[R\left((\hat{q}^{-}_{\mathrm{B/I}})^{*}\right)\ \ 0_{3\times 3}\right], \tag{94}$$

where $\hat{q}_{\mathrm{B/I}}$ is an output of the attitude part of the SQV-AEKF.

In summary, for the measurement update of the position part of the SQV-AEKF, the Kalman gain is calculated from Eq. (10), whereas the optimal Kalman state update is calculated from Eq. (8) as

$$\Delta^{\star}\hat{x}_6(t_k) \triangleq \begin{bmatrix} \Delta^{\star}\overline{\hat{r}}^{\mathrm{B}}_{\mathrm{B/I}} \\ \Delta^{\star}\overline{\hat{b}}_v(t_k) \end{bmatrix} = K_{6\times 3}(t_k)(\overline{r^{\mathrm{I}}_{\mathrm{B/I},m}(t_k)} - \overline{\hat{r}^{\mathrm{I},-}_{\mathrm{B/I}}(t_k)}). \tag{95}$$

The estimate of the state at time t_k after the measurement is then calculated from $\overline{\hat{b}}^{+}_{v}(t_k) = \overline{\hat{b}}^{-}_{v}(t_k) + \Delta^{\star}\overline{\hat{b}}_v(t_k)$ and $\overline{\hat{r}}^{\mathrm{B},+}_{\mathrm{B/I}}(t_k) = \overline{\hat{r}}^{\mathrm{B},-}_{\mathrm{B/I}}(t_k) + \Delta^{\star}\overline{\hat{r}}^{\mathrm{B}}_{\mathrm{B/I}}$. Finally, the covariance matrix of the state immediately after the measurement at t_k is computed from Eq. (13).

As before, when position measurements are available, but linear velocity measurements are not, estimates of $v^{\mathrm{B}}_{\mathrm{B/I}}$ can be determined by setting $v^{\mathrm{B}}_{\mathrm{B/I},m}$ and $\overline{Q}_v$ to zero, and by increasing $\overline{Q}_{b_v}$ if necessary.

Acknowledgments

This work was supported by the AFRL research award FA9453-13-C-0201. The authors would also like to thank Landis Markley for his encouragement and insightful suggestions.

References

[1]Lefferts, E., Markley, F., and Shuster, M., "Kalman Filtering for Spacecraft Attitude Estimation," *Journal of Guidance, Control, and Dynamics*, Vol. 5, No. 5, September-October 1982, pp. 417–429.

[2]Crassidis, J. L., Markley, F. L., and Cheng, Y., "Survey of Nonlinear Attitude Estimation Methods," *Journal of Guidance, Control, and Dynamics*, Vol. 30, No. 1, January-February 2007, pp. 12–28.

[3]Zanetti, R., Majji, M., Bishop, R. H., and Mortari, D., "Norm-Constrained Kalman Filtering," *Journal*

of Guidance, Control, and Dynamics, Vol. 32, No. 5, September-October 2009, pp. 1458–1465.

[4]Markley, F. L., "Attitude Error Representations for Kalman Filtering," *Journal of Guidance, Control, and Dynamics*, Vol. 26, No. 2, March-April 2003, pp. 311–317.

[5]Markley, F. L., "Attitude Estimation or Quaternion Estimation?" *Advances in the Astronautical Sciences*, Vol. 115, 2003, pp. 113–127.

[6]Markley, F. L., "Attitude Filtering on SO(3)," *The Journal of the Astronautical Sciences*, Vol. 54, No. 3 and 4, July-December 2006, pp. 391–413.

[7]Filipe, N. and Tsiotras, P., "Rigid Body Motion Tracking Without Linear and Angular Velocity Feedback Using Dual Quaternions," *European Control Conference*, IEEE, Piscataway, NJ, Zürich, Switzerland, July 17-19 2013, pp. 329–334.

[8]Filipe, N. and Tsiotras, P., "Adaptive Position and Attitude-Tracking Controller for Satellite Proximity Operations Using Dual Quaternions," *Journal of Guidance, Control, and Dynamics*, 2014, DOI: 10.2514/1.G000054.

[9]Dimentberg, F. M., "The screw calculus and its applications in mechanics," Tech. Rep. FTD-HT-23-1632-67, DTIC Document, 1968.

[10]Romano, M., Friedman, D. A., and Shay, T. J., "Laboratory Experimentation of Autonomous Spacecraft Approach and Docking to a Collaborative Target," *Journal of Spacecraft and Rockets*, Vol. 44, No. 1, January-February 2007, pp. 164–173.

[11]Mourikis, A. I., Trawny, N., Roumeliotis, S. I., Johnson, A. E., Ansar, A., and Matthies, L., "Vision-Aided Inertial Navigation for Spacecraft Entry, Descent, and Landing," *IEEE Transactions on Robotics*, Vol. 25, No. 2, April 2009, pp. 264–280.

[12]Kim, S.-G., Crassidis, J. L., Cheng, Y., Fosbury, A., and Junkins, J. L., "Kalman Filtering for Relative Spacecraft Attitude and Position Estimation," *Journal of Guidance, Control, and Dynamics*, Vol. 30, No. 1, January-February 2007, pp. 133–143.

[13]Goddard, J. S., *Pose and Motion Estimation from Vision Using Dual Quaternion-based Extended Kalman Filtering*, Ph.D. thesis, The University of Tennessee, Knoxville, 1997.

[14]Bayro-Corrochano, E. and Zhang, Y., "The Motor Extended Kalman Filter: A Geometric Approach for Rigid Motion Estimation," *Journal of Mathematical Imaging and Vision*, Vol. 13, No. 3, December 2000, pp. 205–228.

[15]Zu, Y., Lee, U., and Dai, R., "Distributed Motion Estimation of Space Objects Using Dual Quaternions," *AIAA/AAS Astrodynamics Specialist Conference*, No. 2014-4296, San Diego, CA, August 4-7 2014.

[16]Lewis, F. L., *Optimal Estimation*, chap. 3.7 Discrete Measurements of Continuous-Time Systems, John Wiley & Sons, Inc., USA, 1986, pp. 185–191.

[17]Filipe, N. and Tsiotras, P., "Adaptive Model-Independent Tracking of Rigid Body Position and Attitude Motion with Mass and Inertia Matrix Identification using Dual Quaternions," *AIAA Guidance, Navigation, and Control Conference*, AIAA 2013-5173, Boston, MA, August 19-22 2013.

[18]Han, D., Wei, Q., Li, Z., and Sun, W., "Control of Oriented Mechanical systems: A Method Based on Dual Quaternions," *Proceeding of the 17th World Congress, The International Federation of Automatic Control*, International Federation of Automatic Control, Laxenburg, Austria, Seoul, Korea, July 6–11 2008, pp. 3836–3841.

[19]Hamilton, W., *Elements of Quaternions*, Longmans, Green, & Company, London, 1866.

[20]Han, D.-P., Wei, Q., and Li, Z.-X., "Kinematic Control of Free Rigid Bodies Using Dual Quaternions," *International Journal of Automation and Computing*, Vol. 5, No. 3, July 2008, pp. 319–324.

[21]Wang, J. and Sun, Z., "6–DOF robust adaptive terminal sliding mode control for spacecraft formation flying," *Acta Astronautica*, Vol. 73, April-May 2012, pp. 676–87.

[22]Wu, Y., Hu, X., Hu, D., Li, T., and Lian, J., "Strapdown Inertial Navigation System Algorithms Based on Dual Quaternions," *IEEE Transactions on Aerospace and Electronic Systems*, Vol. 41, No. 1, January 2005, pp. 110–132.

[23]Filipe, N. and Tsiotras, P., "Simultaneous Position and Attitude Control Without Linear and Angular Velocity Feedback Using Dual Quaternions," *American Control Conference*, IEEE, Piscataway, NJ, Washington, DC, June 17-19 2013, pp. 4815–4820.

[24]Cho, D.-M., Tsiotras, P., Zhang, G., and Holzinger, M. J., "Robust Feature Detection, Acquisition and Tracking for Relative Navigation in Space with a Known Target," *AIAA Guidance, Navigation, and Control Conference*, AIAA 2013-5197, Boston, MA, August 19-22 2013.

[25]Tsiotras, P., "ASTROS: A 5DOF Experimental Facility for Research in Space Proximity Operations," *AAS Guidance and Control Conference*, No. 2014-114, Breckenridge, CO, January 31 - February 5 2014.

[26]Cho, D.-M., Jung, D., and Tsiotras, P., "A 5-DOF Experimental Platform for Spacecraft Rendezvous and Docking," *AIAA Infotech @ Aerospace Conference*, Seattle, WA, April 6–9 2009, AIAA Paper 2009-1869.